Chemical Looping Systems for Alternative Fuel Production and Processing: Advancements to STWS, SMR, the Contact Process and the Sulphur-Iodine Cycle

Nicholas Singstock

Dr. Liang-Shih Fan

April 10th, 2017

WILLIAM G. LOWRIE DEPARTMENT OF CHEMICAL AND BIOMOLECULAR ENGINEERING

THE OHIO STATE UNIVERSITY

Abstract:

The field of alternative energy could be seen as analogous to a deep oil well in that there is a vast amount of potential just waiting to be discovered, however an initial capital investment will need to be made in order to extract this energy. For now, this investment lies in both research and infrastructure, since most of the current issues regarding substitutes for coal and oil rely on their economic viability. The current methods for producing clean energy and fuels will need to be continually improved until they become competitive. Several examples of efficiency and material improvements have been described herein. Using FactSage and thermodynamic minimization, a strong conceptual foundation has been developed for a total of seven chemical looping reaction pathways with the potential to improve the efficiency of producing fuels such as methane and hydrogen, as well as industrial chemicals such as sulphuric acid. These include multiple cycles for hydrogen, methane and sulphuric acid production based on aluminum cerium oxide, an ameliorated sulphur-iodine cycle using silver bromide photodecomposition, and various catalytic improvements for methane reforming and steam methane reforming. Experimental verification should be performed for the proposed reaction pathways in order to determine their potential for actualization.

Table of Contents

Introduction

The global energy consumption rises every year and shows no indications of stopping anytime soon[1]. If these demands continue to be met with coal and gasoline, as they have been since the industrial revolution, then the results could be catastrophic for the environment. Maintaining the current rate of greenhouse emissions is predicted to lead to increased sea levels, an increased global temperature, increased ocean acidity, shifting ecosystems and worsening air quality, the combination of which will significantly affect societies' abilities to maintain adequate food and water supplies for their citizens[2]. On the other hand, producing clean fuel and electricity still faces the issue of being economically competitive with fossil fuels, and it has become increasingly evident that most individuals cannot be relied upon to make responsible, long-term choices for the betterment of society. Since storage of large amounts of electricity still faces a shortcoming in modern battery technology, the near-term goals of environmentally-friendly energy should be focused on efficient fuel production and use. A paragon of clean fuels is hydrogen, which in its compressed form at 700 bar has over triple the energy density of gasoline by mass, and the bane of researchers for many decades has been finding a way of producing hydrogen from water without performing electrolysis. This is because splitting water in to its constituent elements using solar-electricity is only about 16% efficient[3], whereas solar thermal water splitting (STWS) has been shown to have high theoretical efficiencies but also requires temperatures approaching 2000°C[4]. As a result of these shortcomings, around 95% of the hydrogen produced in the United States comes from methane reforming and steam methane reforming (SMR)[5]. Unfortunately, methane is still a hydrocarbon fuel, and even though it is producing hydrogen, SMR also produces a mixture of carbon dioxide and carbon monoxide. Carbon monoxide is used industrially, in a mixture with hydrogen known as syngas, to produce longer chain hydrocarbon molecules such as ethanol via Fischer-Tropsch synthesis[6], but carbon dioxide has minimal industrial value and is almost always a waste product. Due to the commercial viability of SMR, significant efficiency improvements have already been made, bringing carbon dioxide emissions down to only 13 percent above their theoretical minimum[7]. Nevertheless, two areas in modern SMR technology which could benefit from improvement would be decreasing the high heat of operation, 700-1000°C[5], and decreasing the amount of carbon dioxide in the syngas so that it doesn't need to be removed downstream. A simple steam methane reforming process is shown in Figure 1.

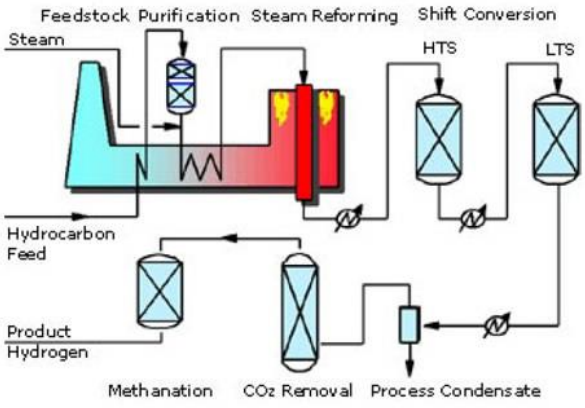

Figure 1: Basic schematic for an SMR process[8].

Hydrogen may provide the foundation for the future of energy production and distribution, therefore efficient and responsible production of it are a pivotal concern. While SMR is a significant step towards alternative fuel production, it can still be improved upon. Chemical looping is a way of recycling the products from one reaction by using them as the reactants for another reaction. In terms of hydrogen production from water, a simple STWS chemical looping cycle would look similar to Figure 2, below, where a metal is oxidized by water, producing hydrogen, and then the metal oxide is reduced at high temperatures back to the metal.

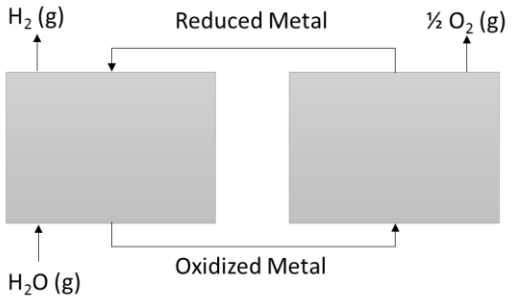

Figure 2: A basic chemical looping cycle which receives water as an input and produces hydrogen and oxygen.

There are multiple benefits to using a chemical looping cycle; primarily, there are very few continuous material inputs required after the system has been constructed, in the case of the cycle in Figure 2 the only input is water. Commonly, one reactor will be endothermic while the other is exothermic, so a heat transfer from one reactor to the other can occur. If the endothermic reaction were to take place at a higher temperature than the exothermic reaction, then a heat pump could be used to convert some of the low temperature waste heat in to high temperature heat for the endothermic reaction. The use of chemical looping in already developed chemical plants could be a useful addition to make processes more efficient and even produce additional value from the system. For example, a metal oxide can be used for additional selectivity during methane reforming, and the reduced metal could be oxidized in air, or, for added value in the system, it could be oxidized by water, producing hydrogen as a byproduct. In this way, chemical looping can provide added value to an already functional chemical plant.

Sulphuric acid, as a second example, is the most highly produced chemical on the planet[9], and the vast majority of it is produced through the contact process. In this process, raw sulphur is oxidized in air, producing sulphur dioxide, which is then further oxidized to sulphur trioxide before being absorbed in to high concentration sulphuric acid. The first step of this process, oxidation of sulphur, is highly exothermic, producing large amounts of heat which can be recycled to other parts of the process. Rather than oxidation in air however, sulphur could be oxidized with a metal oxide which could then be used to reduce water in a second reactor, as depicted in Figure 3. This chemical looping process could be used to produce twice as much hydrogen as sulphuric acid for a relatively low additional cost. This is a huge amount of hydrogen considering global sulphuric acid production in 2013 was over 230 million metric tons[10]. If hydrogen was produced concurrently, this would surmount to over 18 million metric tons of hydrogen per year which is about a third of the annual 50 million tons of hydrogen produced globally, according to a 2013 report by the United States Department of Energy[11].

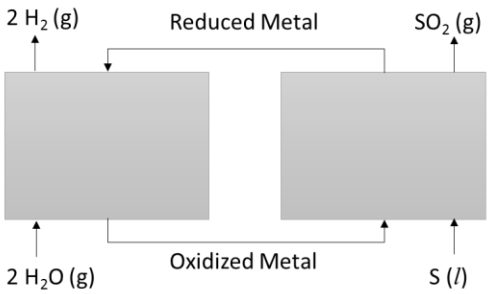

Figure 3: A chemical looping cycle which recieves sulphur and water as inputs and produces hydrogen and sulphur dioxide. The sulphr dioxide can be further transformed in to sulphuric acid downstream.

This adaptation to the contact process which produces hydrogen alongside of sulphuric acid serves as the basis for two of the developed systems, both using aluminum cerium oxide as the chemically looped metal oxide complex. The rest of the system relies on the latter half of the contact process beginning at the catalytic converter; the contact process is graphically represented in Figure 4 for comparison.

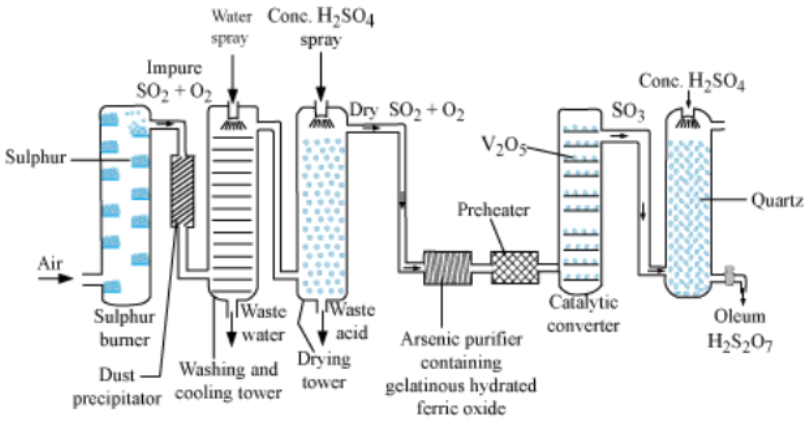

Figure 4: Schematic of the contact process[12].

The sulphur-iodine cycle was developed in 1970 by General Atomics[13] as a possible way of producing hydrogen through STWS relying on sulphuric acid and hydroiodic acid. This system, as seen in Figure 5, is a chemical looping cycle between three reactors which produces hydrogen and oxygen from water. There are two major flaws with this process however. Primarily, the sulphuric acid thermal decomposition occurs at high temperatures so advanced materials would need to be used in order to contain this caustic chemical at the necessary temperatures. Additionally, the thermal decomposition of hydroiodic acid is not very favorable and the decomposition products need to be continually removed from the system in order to shift the equilibrium towards product formation. This poses a separation issue because at the decomposition temperature for hydroiodic acid, both the products and reactants are gaseous. Both of these issues were theoretically resolved in the ameliorated sulphur-iodine cycle.

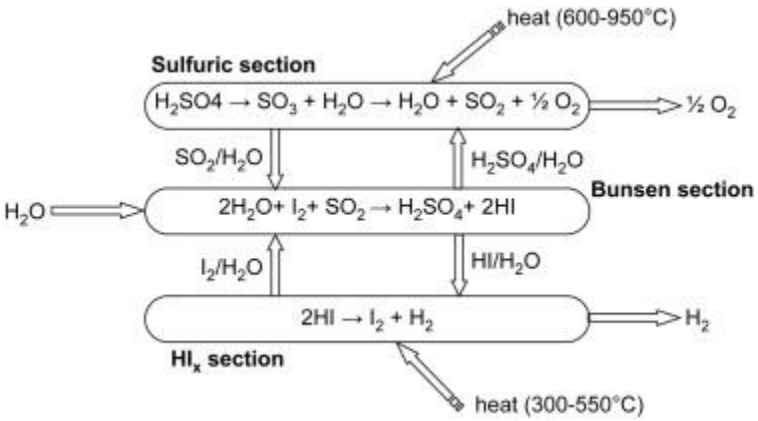

Figure 5: Schematic of the sulphur-iodine cycle[14].

This cycle is somewhat unique in comparison to most of the other proposed STWS cycles in that it operates at relatively low temperatures which are achievable through solar thermal energy alone. Another large perk to this system though is that it consists solely of liquid and gas phases and therefore the transport of materials between reactors is more industrially simple.

A total of seven reaction pathways for chemical looping systems are presented and defended herein. These fall in to three general categories: aluminum cerium oxide cycles, solar thermal water splitting and methane reforming. The aluminum cerium oxide cycles can be further broken down in to solar thermal water splitting, thermo-electric water splitting and contact process adaptations. The primary function of all of the proposed cycles is to serve as more efficient and clean possibilities for fuel generation.

Methodology

All of the chemical looping reaction pathways were developed and verified using FactSage, a thermodynamic-minimization software which provides a strong prediction of product formation given a certain set of input materials. This software was used to make all of the plots and graphs which have been included. Outside of this software, additional research was focused on literature review and new applications of developed reactions. FactSage was used as a screening tool in order to determine the favorability of different reaction pathways. It provided a quick and efficient way of analyzing hundreds of different metal complex systems, the best of which were kept while the vast majority were discarded.

For the purpose of SMR catalyst development, over 170 transition metals and metal complexes were investigated as potential oxidizers of solid carbon. Those metal oxides which could be reduced by carbon at temperatures below 1000°C were kept, while the rest were deemed to be too thermodynamically stable were removed from screening. Those materials which acted as carbon oxidizers were added to a modified Ellingham Diagram, seen below in Figure 6. This graph details the effect of temperature on the Gibb's Free Energy of a reaction; those reactions which have a lower, more negative, Gibb's Free Energy change are more favorable. In Figure 6, all of the plotted reactions involve the oxidation of a reduced metal, or reduced complex of metals, with half of a mole of oxygen. Since all of the reactions

are of the same nature, oxidation with one-half mole of diatomic oxygen, the favorability of one reaction over another is easily determined by examining which reaction has a lower ΔG at the given temperature.

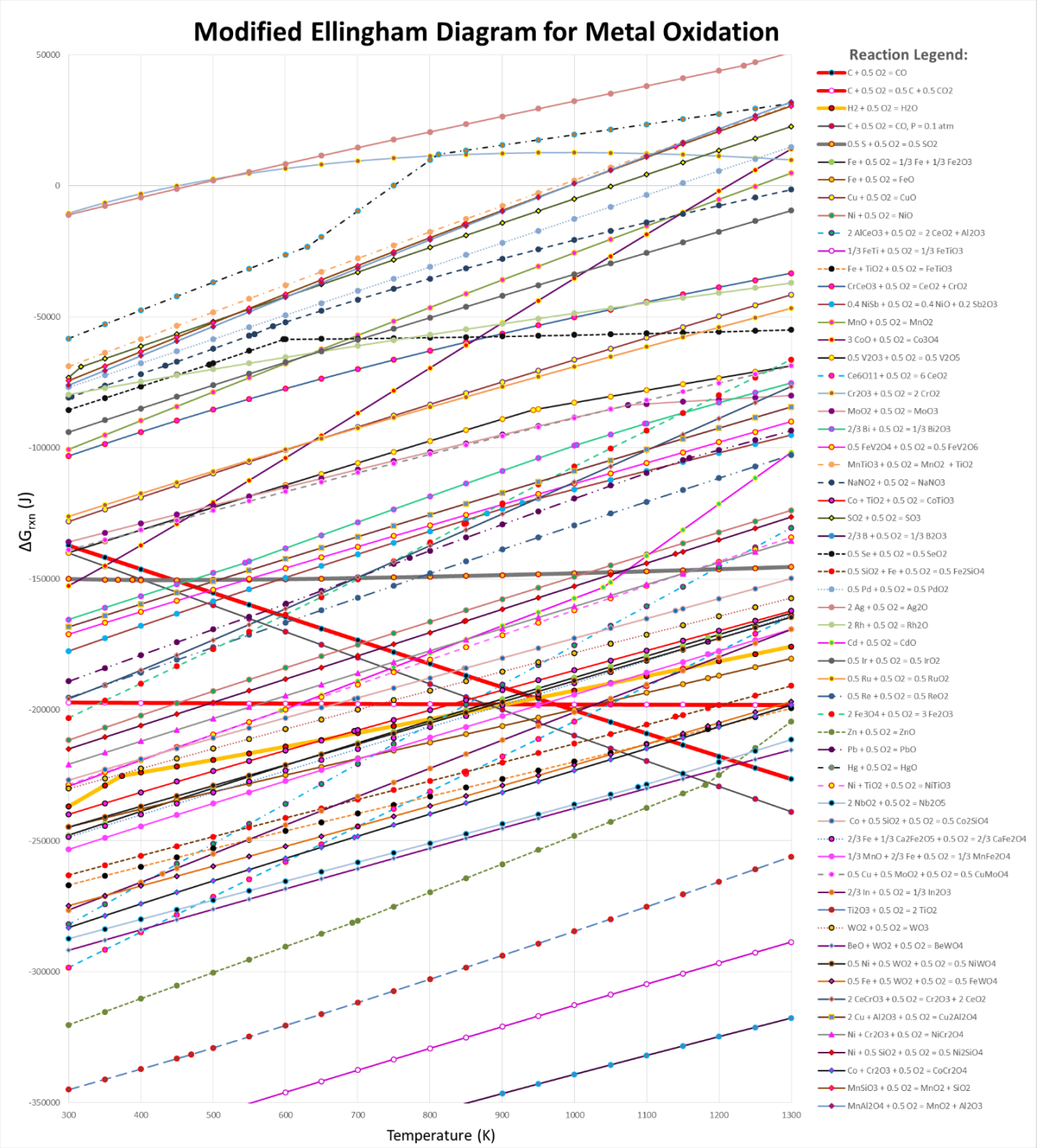

Figure 6: Modified Ellingham Diagram depicting oxidation reactions for various metal and metal-complex systems. Reactions which are higher on the chart are less thermodynamically stable and those which are lower on the chart have a more negative ΔG_{rxn} and are therefore more stable. Materials which are lower on the diagram can theoretically reduce materials which are higher on the diagram. Thermodynamic data tables can be found in Appendix H.

For clarification, the equals-sign used in the legend can be thought of as a reaction arrow separating the reactants, on the left, from the products on the right. The intersection of two lines on this diagram can be thought of as potential reactions, or places where one reaction is favorable over another. Figure 6, therefore, provided the framework for discovering a large number of possible oxidation-reduction reaction pathways. There are still caveats, however, as side reactions can occur which deviate from the expected reaction pathway. As a result, Figure 6 functions as a preliminary screening tool, and those reaction pathways which appear favorable must be further investigated using FactSage in order to predict the actual reaction products. The largest limitation to FactSage's predictive capability is its lack of reaction kinetic data; as a result, experimental confirmation is required as a final step in verifying the proposed reaction pathways.

For easier reference, the oxidation reactions for hydrogen and carbon have been plotted using thick yellow and red lines, respectively. The investigated temperature range started at 300 K, around room temperature, and was capped at 1300 K. Temperatures below 300 K were eliminated from screening because of the high probability of slow reaction kinetics, and temperatures above 1300 K (1027°C) were considered to be too high for SMR and STWS. For STWS purposes, the goal was to discover a lower-temperature reaction pathway which would start with the reduction of water to hydrogen, and end with the reduction of a metal in air. For reduction in air to be thermodynamically possible, the ΔG_{rxn} must be positive. Special focus was placed on those materials which had a steeper slope, as they more quickly approached $\Delta G_{rxn} = 0$ with increasing temperature. Specific attention was placed on aluminum cerium oxide, $AlCeO_3$, as it had the largest slope of any material which could reduce water at lower temperatures. As a result, it was the water-splitting material which was most readily reduced at 1300 K. For SMR purposes, the main area of importance on Figure 6 is from about 900 K to 1300 K where carbon monoxide formation becomes favorable to carbon dioxide formation, given a 1:1 carbon to oxygen ratio. Those materials which fall in this range are theoretically capable of producing a higher-purity syngas with lower carbon dioxide concentrations. Additional screening criteria were also considered. Generally, the reaction should occur at higher temperatures and have at least one fluid phase reactant so that the kinetics of the reaction will likely be fast. Furthermore, the product species should be different phases so that they are easily separable.

This method for efficiently screening a large number of materials to develop a significant database of thermodynamically-feasible reactions is, perhaps, more significant than the actual systems which were developed. Further expansion upon this methodology could involve plotting multiple types of reactions with a myriad of metals and metal complexes in order to map a large number of complex theoretical reaction pathways. As before, these developed reaction pathways would still need to undergo additional verification steps in order to determine their validity. Not all of the proposed cycles were developed in this manner however; specifically, the alterations to the sulphur-iodine cycle were developed during analysis of the existing flaws with current STWS technology.

Aluminum Cerium Oxide: Two-Reactor Solar Thermal Water Splitting

Simplicity is key. For a chemical process, this means minimizing the number of reactors and the number of steps in the process. Figure 2 shows a two-reactor chemical looping cycle which is the ultimate form of simplicity for an STWS method. Figure 8, below, depicts a very similar, two-cycle chemical loop which relies on aluminum cerium oxide to carry oxygen between the reducer and the oxidizer. A highly simplified version of the modified Ellingham Diagram is presented in Figure 7 to demonstrate the theoretical reaction pathway.

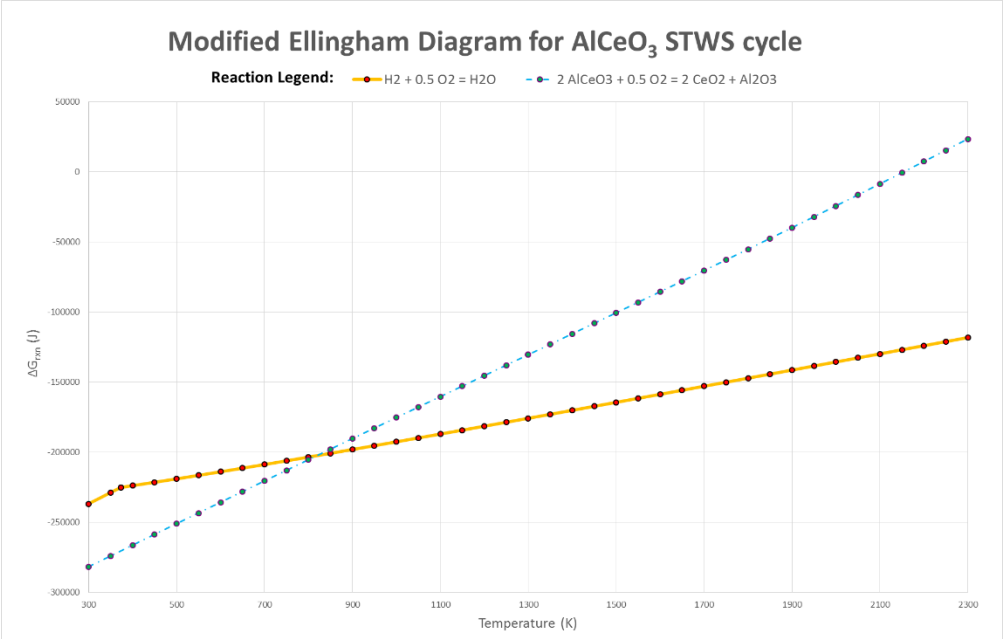

Figure 7: Simplified Ellingham Diagram representing the oxidation and reduction steps of the two-cycle STWS chemical loop.

Using Figure 7 as a reference, reaction conditions can be determined. As shown, below 800 K (527°C), water can be reduced to hydrogen by $AlCeO_3$ which is oxidized to cerium(IV) oxide and aluminum(III) oxide. The second reaction, reduction of the metal complex to re-form $AlCeO_3$, occurs around 2114 K (1841°C) at the point where the aluminum cerium oxide ΔG_{rxn} becomes positive. This system is similar in nature to the aptly-named Cerium(IV) oxide-Cerium(III) oxide cycle, however it releases oxygen at a lower temperature. Both systems exploit the oxidation state shift of cerium from +4 to +3 at high temperatures. The major difference is that, at 0.1 atm, aluminum cerium oxide reduction occurs at around 1775°C, whereas the strictly cerium STWS cycle reduction occurs at 2105°C according to FactSage. This temperature can be further lowered by decreasing the system pressure and by sweeping air through the reducer, both of which lower the partial pressure of oxygen in the system. These implementations can be seen in Figure 8, the proposed STWS chemical looping cycle.

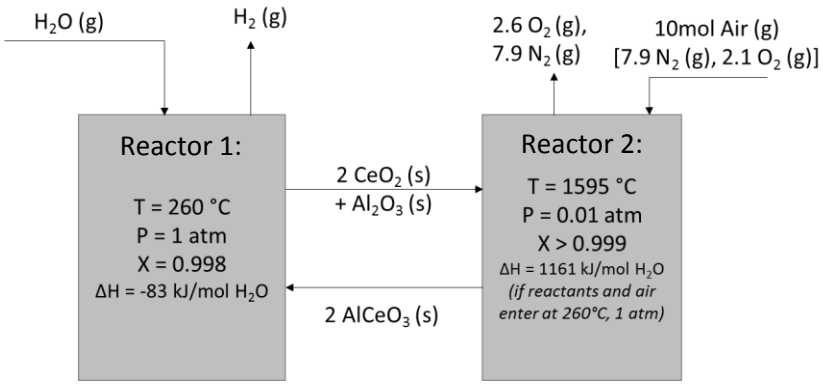

Figure 8: Aluminum cerium oxide based STWS chemical looping cycle.

Equation 1 and Equation 2 show the oxidation and reduction reactions, respectively, of the aluminum cerium oxide metal complex.

Equation 1: Oxidation of aluminum cerium oxide in water, producing hydrogen at 260°C.

$$H_2O(g) + 2\ AlCeO_3(s) \rightarrow\ H_2(g) + 2\ CeO_2(s) + Al_2O_3(S)$$

Equation 2: Reduction of aluminum cerium oxide via thermal decomposition at high temperature.

$$2\ CeO_2(s) + Al_2O_3(s) \rightarrow 2\ AlCeO_3(s) + \frac{1}{2}\ O_2(g)$$

This system, like others, has its advantages and shortcomings. Both reactions have high predicted conversions, according to FactSage. The thermodynamic verification of the reaction conversions and enthalpies can be seen in Appendix A. This STWS cycle also operates at a relatively low temperature when compared to other cycles of a similar nature. Another benefit to the system is that both reactions produce a solid and a gas phase which are easily separated. The heat produced in the first reactor can be used to partially heat the sweeping air stream, as can the hot products leaving the second reactor. The rest of the heat would be obtained by concentrating solar thermal energy. As for the shortcomings, the temperature in the second reactor is still likely to be too high to implement industrially, and the highly endothermic nature of heating the input materials of the second reactor to nearly 1600°C is undesirable. Unfortunately due to these shortcomings, this system would likely not be industrially-viable. If the temperature could be further reduced to around 1100°C, however, then it would be highly competitive with current SMR processes due to its similar temperature range and its lack of methane as an input material. Lower temperatures in the second reactor could potentially be achieved by doping the metal complex in order to destabilize its lattice structure or by further reducing the partial pressure of oxygen in the system.

Aluminum Cerium Oxide: Hybrid Thermo-Electric Sulphur Dioxide Reduction

In order to reduce the aluminum cerium metal complex at lower temperatures, it can be reacted with liquid or gas phase sulphur. Figure 9 shows a simplified version of the modified Ellingham Diagram in Figure 6 which includes the line for sulphur oxidation to sulphur dioxide. This system is conceptually similar to Figure 3, which depicts a two-reactor cycle that receives water and sulphur as inputs and produces hydrogen and sulphur dioxide. The sulphur dioxide cannot be released in to the air because of its environmental impact, and so it must be used. It was theorized that electrolysis could be used to reduce

the sulphur dioxide back to liquid sulphur and oxygen. Since the $\Delta G_{formation}$ of sulphur dioxide is about 90 kJ less than that of water, it would require less electricity to perform electrolysis on sulphur dioxide. This cycle could therefore serve as a lower energy way of producing hydrogen via electrolysis. An additional energy cost would be incurred by the heating and pumping of materials in the system, and these exact energy costs would be dependent upon the system design. Since solar thermal energy is more theoretically efficient than photovoltaics though, the introduction of solar thermal energy should serve to decrease the overall energy cost of water splitting. A chemical process modeling software could be used to determine if the overall energy input would be more efficient than direct electrolysis of water.

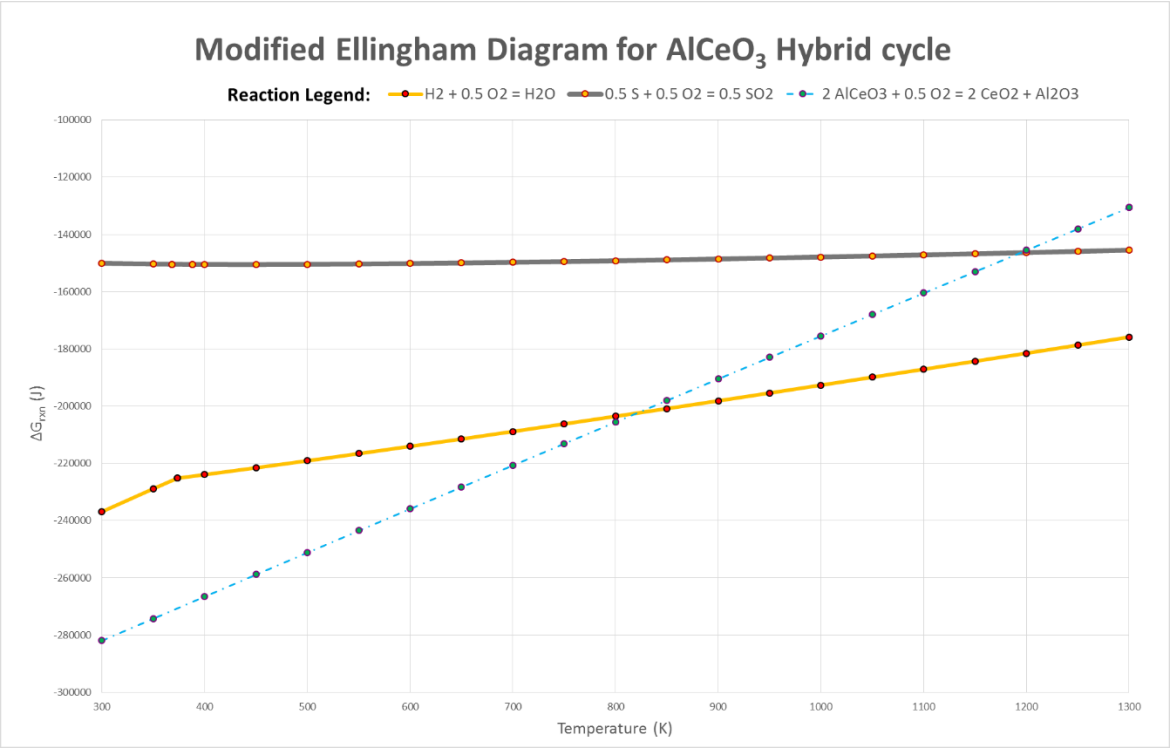

Figure 9: Simplified Ellingham Diagram showing the oxidation and reduction conditions for the hybrid thermo-electric cycle.

There are two important transitions in Figure 9, the first is below 800 K where, similar to before, aluminum cerium oxide is capable of reducing water to hydrogen, and the second is above 1200 K (927°C) where elemental sulphur is capable of reducing aluminum cerium oxide. Of all of the metal complexes studied, Aluminum cerium oxide was unique in its ability to perform both of these reactions within the investigated temperature range. Equation 1, oxidation of $AlCeO_3$ in water, in addition to Equations 3 and 4, illustrate the three primary reactions occurring in this chemical looping system.

Equation 3: Reduction of aluminum cerium oxide with sulphur, producing sulphur dioxide at 1080°C.

$$4\ CeO_2(s) + 2\ Al_2O_3(s) + \frac{1}{2}S_2(g) \rightarrow 4\ AlCeO_3(s) + \ SO_2(g)$$

Equation 4: Electrolysis of sulphur dioxide in to its constituent elements.

$$SO_2\ (g) \rightarrow S\ (l) + \ O_2\ (g)$$

It is important that the electrolysis of sulphur dioxide occur above the melting point of sulphur, 115°C, so that solid sulphur is not produced, as it would form on the electrodes, hindering their ability to

perform further electrolysis. Electrolysis of liquid sulphur dioxide has previously been studied[15], however at the specified 115°C, sulphur dioxide is a gas so electrolysis would be more complicated. No previous investigation of gas-phase sulphur dioxide electrolysis could be found in published literature. Consequently, the feasibility of this cycle is somewhat unknown due to a lack of experimental data or literature confirmation. The theoretical hybrid cycle can nonetheless be seen in Figure 10.

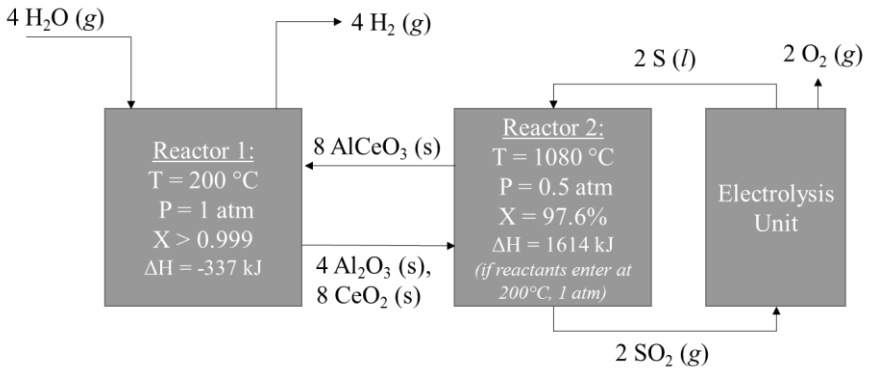

Figure 10: Hybrid thermo-electric water-splitting cycle using $AlCeO_3$.

As before, the only inputs to the system are heat and water, and the only products are hydrogen and oxygen. The reaction conversions are very high, and the products in each reactor are easily separable. The temperature in the second reactor is feasible for solar thermal energy, however there is a relatively large temperature swing between the two reactors which would decrease the overall efficiency of the chemical looping cycle. The reaction in the second reactor is highly endothermic, however this does account for heating the input materials to reactor conditions from 200°C.

A further advancement of this cycle would be to make it entirely solar thermal energy based. This could theoretically be done by reducing the sulphur dioxide with a second metal complex. As shown in Figure 11, it is theoretically possible to reduce sulphur dioxide back to elemental sulphur using cobalt (II) oxide, which could then be reduced in air around 950°C. This cycle would require a total of four reactors, and would have three materials being looped.

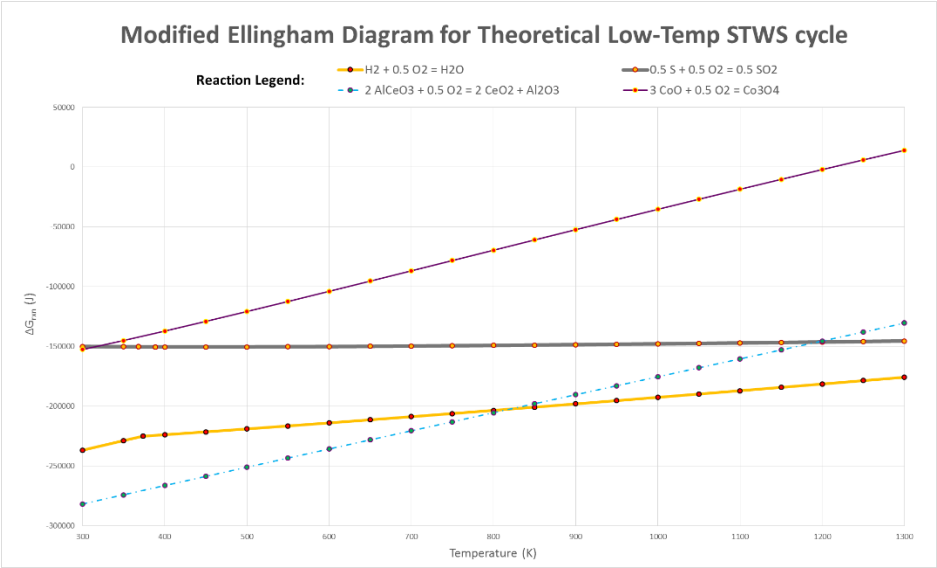

Figure 11: Theoretical four-reactor chemical looping system for low temperature STWS.

There are a couple of fundamental issues with this cycle however, the primary one being that cobalt (II) oxide reacts with sulphur dioxide to form cobalt sulfate. Aside from this critical flaw, the temperature for sulphur reduction would need to be higher so that the elemental sulphur produced was not in a solid phase, and the reaction kinetics would be fast enough to implement industrially. Sulphur in a gas or liquid phase would be easier to separate from the oxidized cobalt. Nonetheless, this is a promising development in STWS technology, as it demonstrates that there may be materials which could be used in this cycle. An ideal material would be capable of reducing sulphur dioxide to liquid sulphur at temperatures above 115°C, auto-thermally reducing in air at reasonable temperatures for STWS, below about 1000°C, and would have fast kinetics for both reactions. A material of this nature could be a viable solution to low-temperature STWS chemical looping in a four reactor system. No material fitting these specifications was discovered during the screening process however.

Aluminum Cerium Oxide: Hydrogen Production in the Contact Process

Another possibility for the sulphur dioxide produced in the hybrid cycle would be to use it for sulphuric acid production. The first two reactors from the hybrid thermo-electric cycle would remain the same, however instead of reducing the sulphur dioxide via electrolysis, it would be sent to the latter half of the contact process. In this way, the overall system would receive water, sulphur and oxygen as inputs, and produce hydrogen and sulphuric acid. Figure 12 demonstrates a conceptual system design for this process. The thermodynamic specifications for the last two reactors, which convert sulphur dioxide to sulphuric acid, are from literature regarding the contact process[16].

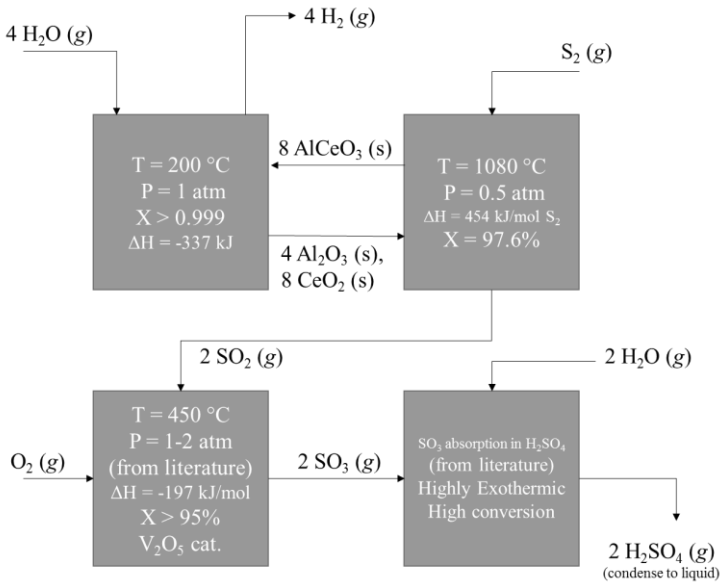

Figure 12: Chemical looping cycle using aluminum cerium oxide and the contact process to produce hydrogen and sulphuric acid.

The last two units, sulphur dioxide oxidation and sulphur trioxide absorption, have been highly refined and optimized for industrial purposes. Consequently, no new developments were added to either of these units. The rationale and reactor specifications for the first two units were expounded upon during analysis of the hybrid thermo-electric system, since both reactors in this system are nearly identical to their counterparts in the hybrid cycle. The only differences are in the second reactor, which has gas-phase

sulphur entering in this system, and the listed ΔH is the enthalpy of reaction, rather than the overall system enthalpy change. Thermodynamic verification of these reactions can be found in Appendix B and C, and the reactions themselves are presented in Equations 1 and 3.

Aside from the first reactor in Figure 12 which is not at all present in the contact process, the conditions for the second reactor, producing sulphur dioxide from sulphur, have also changed. In the contact process, this step occurs through burning liquid sulphur in air, a process that generates a significant amount of heat, and reactor temperatures ranging from 1000-1600°C[17]. As a result, current industrial sulphur oxidation reactors should suffice to meet the temperature proposed for this modified contact process. This significantly lowers the capital investment that would be required to update a modern industrial sulphuric acid plant in order to produce hydrogen concurrently. Only one additional reactor would need to be installed, the first reactor in Figure 12, which serves to reduce water to hydrogen. Additionally, a pumping mechanism would need to be implemented in order to cycle the aluminum cerium oxide if the process is to run continuously. The heat produced in the first reactor could also be used to produce steam, and thus electricity, in order to provide part of the energy required to pump the metal complex. The heat required to achieve 1080°C in the second reactor could be achieved by solar thermal energy, however this would require additional capital investment and would only work in certain climates. A current industrial plant desiring to modify their existing system would therefore be more inclined to use heaters in order to achieve this temperature.

Overall, the implications of implementation of the modified contact process would be significant. Large scale application could result in the production of up to 18 million metric tons of hydrogen annually and potentially lower hydrogen production costs to an economically-competitive point.

Aluminum Cerium Oxide: Methane Production in the Contact Process

This modified contact process can also be altered to produce methane and sulphuric acid rather than hydrogen and sulphuric acid, as seen in Figure 13.

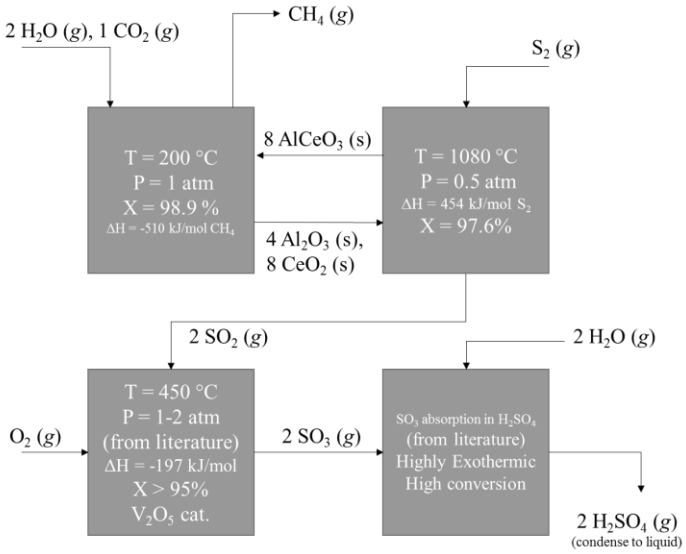

Figure 13: Methane production parallel to sulphuric acid in the modified contact process.

The thermodynamic verification for this process can be seen in Appendix D, and the reactions can be seen in Equations 3 and 5. This process operates similarly to the hydrogen-producing modified contact process, but it creates a single mole of methane rather than four moles of hydrogen. As before, this reaction produces a large amount of energy which can be used to produce electricity for pumping the aluminum cerium oxide between reactors.

Equation 5: Reduction of water and carbon dioxide over aluminum cerium oxide to form methane at 200°C.

$$2\,H_2O(g) + CO_2(g) + 8\,AlCeO_3(s) \rightarrow CH_4(g) + 4\,Al_2O_3(s) + 8\,CeO_2(s)$$

One of the most significant details of this process is that it is, theoretically, carbon negative. It receives carbon dioxide from the environment and converts it in to a carbon-based fuel: methane. The process of converting methane to syngas is already applied industrially in the United States, and syngas can be used to produce longer-chain hydrocarbons, including liquid fuels. Since these fuels would have been produced from carbon dioxide, burning them to produce energy elsewhere would not contribute a net change to the global carbon dioxide production, rather it would be an overall neutral process. The impacts of being able to burn fossil fuels without contributing to carbon dioxide production are huge. Modern transportation vehicles which rely on gasoline power would be able to run on carbon neutral fuel, vastly reducing the impact of the transportation industry on climate change.

This is also beneficial to the sulphuric acid industry in that they can sell their current product, while also selling methane, or syngas, and carbon credits since the process reduces environmental carbon dioxide. Large scale adaptation to existing systems could be used to produce over 35 million tons of methane per year. Since methane transportation is currently uneconomical however, a way of reforming the methane in to liquid fuels would likely need to be added in conjunction with the proposed modifications in order to make the methane production worthwhile. This is an area where more research still needs to be performed. Consequently, it is likely to be more cost-effective to produce hydrogen alongside of sulphuric acid rather than methane.

Ameliorated Sulphur-Iodine Cycle using Silver Bromide Photodecomposition for STWS

Perhaps the largest current issue with the sulphur-iodine cycle is that it relies on the high-temperature thermal decomposition of sulphuric acid. This reaction, which occurs above 800°C[18], would require highly advanced, corrosion-resistant materials in order to enclose. Another possibility, however, is to reduce the sulphuric acid at a lower temperature by reacting it with solid palladium at 400°C. The palladium can then be thermally-decomposed in a separate reactor at 870°C in order to remove oxygen from the system. These reactions can be seen below in Equation 6 and Equation 7, and the thermodynamic verification can be found in Appendix E.

Equation 6: Sulphuric acid reduction with palladium at 400°C.

$$H_2SO_4(g) + Pd(s) \rightarrow SO_2(g) + H_2O(g) + PdO(s)$$

Equation 7: Auto-thermal decomposition of palladium at 870°C.

$$PdO(s) \rightarrow Pd(s) + \frac{1}{2}O_2(g)$$

Another concern with the sulphur-iodine cycle is that thermal decomposition of hydrogen iodide has a low conversion, about 20% according to FactSage[Appendix E], and so additional equilibrium techniques would need to be employed in order to drive the reaction forward, and this would require additional units. Another possibility would be to use bromine in place of iodine, producing hydrobromic acid rather than hydroiodic acid, as seen in Equation 8.

Equation 8: Low temperature reaction of sulphur dioxide, bromine and water to make hydrobromic acid and sulphuric acid[19].

$$2\,H_2O(l) + Br_2(g) + SO_2(g) \rightarrow H_2SO_4(l) + 2\,HBr\,(g)$$

The sulphuric acid can then be reduced over palladium, and the hydrobromic acid can be reacted with solid silver to form silver bromide and hydrogen. The hydrogen gas can be removed from the system, and the silver bromide can be photodecomposed under sunlight to form solid silver and bromine gas; both of these reactions can be seen in Equations 9 and 10, below. This system would therefore rely on water, solar thermal energy and sunlight as inputs to produce hydrogen and oxygen. Some electricity would also be required in order to pump the chemical looping materials between reactors.

Equation 9: Solid silver reacting with hydrobromic acid to form silver bromide and hydrogen.

$$2\,HBr(g) + 2\,Ag(s) \rightarrow H_2(g) + 2\,AgBr(s)$$

Equation 10: Photodecomposition of silver bromide under ultraviolet radiation.

$$2\,AgBr(s) + 2\,hv \rightarrow 2\,Ag(s) + Br_2(g)$$

Thermodynamic verification of Equation 9 can be found in Appendix E; the photodecomposition of silver bromide, however, cannot be simulated in FactSage and therefore comes from literature. Silver bromide, like most silver halides, is light sensitive and is used in traditional photography[20]; as such, silver chloride also works in this cycle. Silver bromide is noted for being more sensitive to light than silver chloride[21], though unfortunately there is almost no kinetic research in to the rate of decomposition or methods for increasing the rate of decomposition, such as concentrating solar energy. The viability of this system in practical application therefore relies heavily on experimental analysis of silver bromide photodecomposition kinetics. If the kinetics of this reaction are practical for industrial use, then this system could serve as a low temperature STWS chemical looping cycle which would rival the temperatures used in modern SMR systems. Without requiring a natural gas feedstock, this system could potentially be more cost-effective than SMR, and therefore lower the production price of hydrogen. The reaction pathway for this system can be seen in Figure 14.

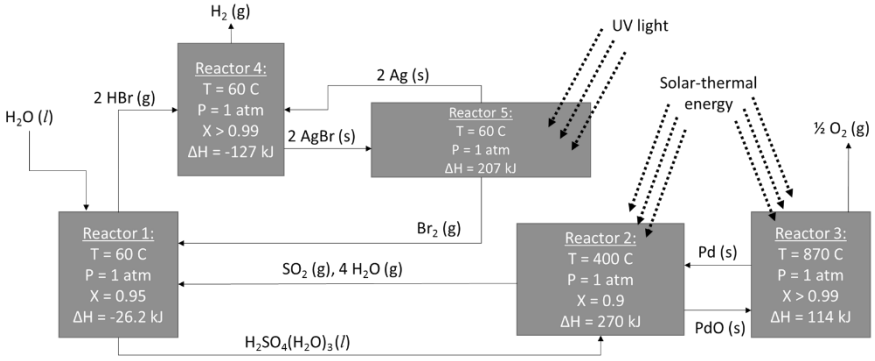

Figure 14: STWS cycle using sulphur-iodine fundamentals ameliorated with silver bromide decomposition and palladium reduction of sulphuric acid.

Silver Iodide is also photosensitive and there has been at least one study in to the kinetics of its photodecomposition. It was determined that silver iodide has "a considerably lower rate"[22] of photodecomposition when compared to other silver halides due to a two-step mechanism which differs from the standard one-step mechanism for other silver halides. The rate of decomposition for silver iodide was slow, on the order of dozens of hours, however methods for accelerating the decomposition were also found, such as adding sulphur dioxide or n-butyl alcohol[22]. It was also found that the surface photodecomposition occurred primarily on the surface of the material, so using finer powders allowed for larger degrees of decomposition[22]. This is nonetheless promising since silver bromide decomposition was implied to decompose much faster than silver iodide, making it more suitable for industrial implementation. The Bunsen Reaction in the standard sulphur-iodine cycle has also been shown to have some issues, primarily that the sulphuric acid and hydroiodic acid layers are slightly miscible and can produce side reactions[23], so utilizing bromine appears to be conceptually superior since this reaction, which has been proven[19], produces gaseous hydrobromic acid that is easily separable from the liquid sulphuric acid.

Low Temperature Steam Methane Reforming with Cadmium Hydroxide

Using Figure 6 as a reference, one particular metal stood out for its oxidative and reductive properties: cadmium. In specific, cadmium is useful in that it forms a hydroxide at temperatures below 130°C, allowing for the generation of hydrogen when elemental cadmium is mixed with water as seen in Equation 11. The simplified, modified Ellingham diagram shown in Figure 15 also serves to elucidate the thermodynamic rationalization of this reaction.

Equation 11: Reduction of water with elemental cadmium at 37°C.

$$8\,H_2O(l) + 4\,Cd(s) \rightarrow 4\,Cd(OH)_2(s) + 4\,H_2(g)$$

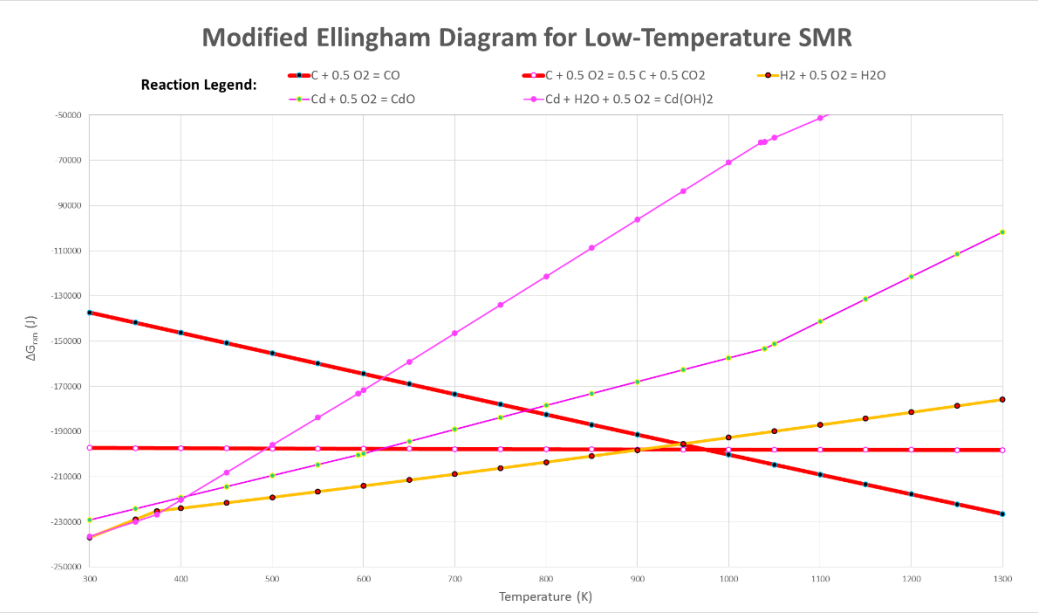

Figure 15: Justification for low temperature SMR process using cadmium and cadmium hydroxide.

Upon heating, the cadmium hydroxide decomposes to cadmium oxide and water at 134°C, and the cadmium oxide can be used to fully oxidize methane to carbon dioxide and water. This reaction, seen in Equation 12, reduces the cadmium oxide to elemental cadmium which can be reacted with water again in order to form more hydrogen.

Equation 12: Oxidation of methane with cadmium oxide at 400°C.

$$CH_4(g) + 4\,CdO(s) \rightarrow 4\,Cd\,(l) + CO_2(g) + 2\,H_2O\,(g)$$

The liquid cadmium can be separated from the gas phase, and the gas phase can be cooled in order to separate the liquid water from the carbon dioxide. This water, in addition to the water produced during cadmium hydroxide decomposition, can be recycled and added to the input water stream that proceeds to react with elemental cadmium. Thermodynamic verification for these reactions can be found in Appendix F. This reaction network combined in a chemical looping cycle can be seen in Figure 16.

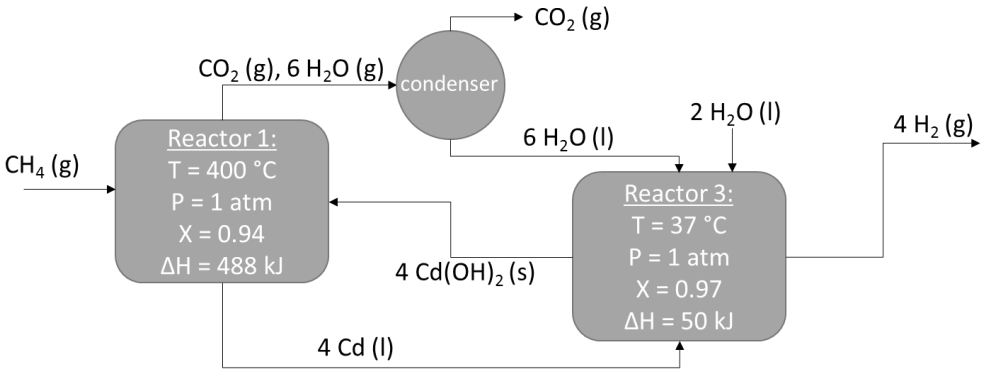

Figure 16: Low-temperature SMR system using cadmium and cadmium hydroxide.

This system has the obvious perk over standard SMR processes in that it operates at a maximum temperature of 400°C rather than conventional industrial SMR processes which operate in the range of 700-1000°C[5]. In addition, four moles of hydrogen are produced per mole of methane, which is more efficient than normal methane reforming processes which produce about three moles of hydrogen per mole of methane. This is due to the fact that this system produces carbon dioxide as opposed to carbon monoxide, so this system, in its current arrangement, would not produce syngas. Unfortunately, due to thermodynamic constraints, carbon monoxide cannot be produced at temperatures below about 700°C unless pressure or equilibrium conditions are exploited. If carbon monoxide production was also desired then the carbon dioxide produced could be added in a 1:1 ratio with methane and basic dry reforming techniques could be used to produce carbon monoxide and hydrogen as seen in Equation 13.

Equation 13: Dry reforming reaction to produce syngas from carbon dioxide and methane above 700°C.

$$CO_2(g) + CH_4(g) \rightarrow 2\,CO(g) + 2\,H_2(g)$$

These two processes could be combined in different ratios in order to produce a large range of syngas compositions. This is beneficial because different ratios of CO:H_2 in syngas are used for producing different hydrocarbons, and the process of combining two gases is far more energy efficient than separating mixed gases. Another advantage to this process is that almost all of the materials being pumped between reactors are in a liquid or gas phase, making them easier to transport. It should be noted that cadmium has known health and environmental risks and, like any toxic chemical, care should be taken

while working with it. As with all of the other reaction pathways though, this system is only proven thermodynamically, and industrial implementation will rely heavily on kinetic, experimental and economic analysis.

Materials for Methane to Syngas Chemical Looping

It has been demonstrated that materials such as iron titanium oxide are able to selectively oxidize methane to high purity syngas with more stability and less byproducts when compared to conventional materials such as nickel oxide, which is a common industrial catalyst for methane reforming[24]. Oxides of cerium have also been demonstrated to produce high purity syngas, however cerium oxide has slow kinetics for methane oxidation[24]. The reason that both of these materials work so well at producing high purity syngas can be explained through the modified Ellingham diagram in Figure 6. Both of these materials fall in the range between carbon dioxide and carbon monoxide oxidation, as seen below in Figure 17, a modified Ellingham diagram including all of the materials which were found to fall in this range as well.

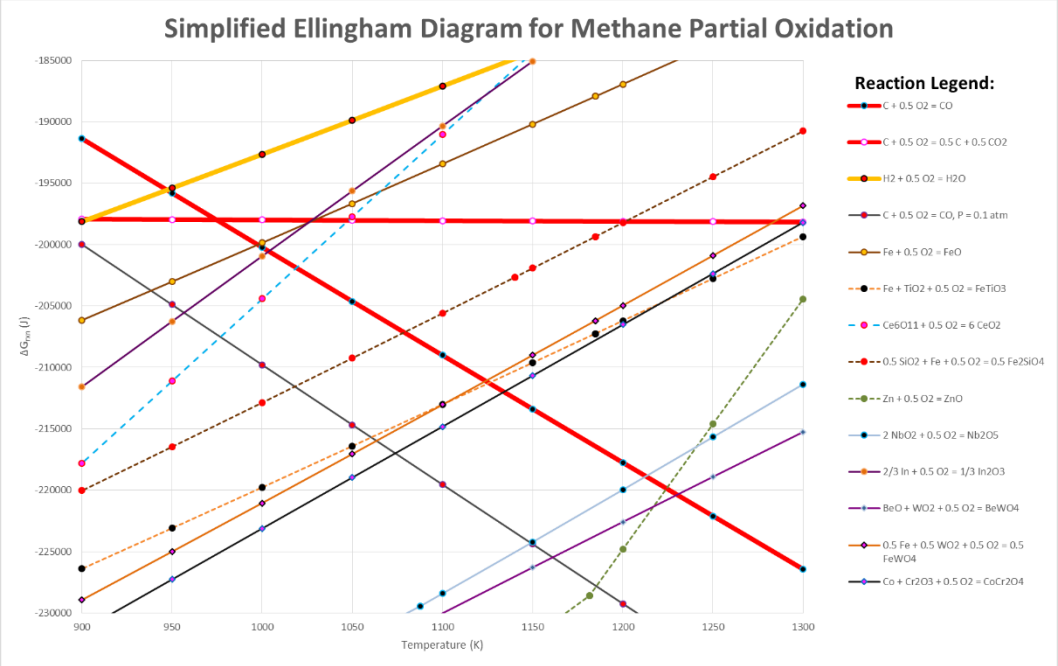

Figure 17: Simplified Ellingham diagram including all of the materials which were found to fall between carbon dioxide and carbon monoxide oxidation.

As seen in Figure 17, cerium oxide and iron titanium oxide both fall within the specified range between carbon dioxide and carbon monoxide. Within this range, materials are able to oxidize carbon to carbon monoxide far more selectively because the metal oxide is more stable than carbon dioxide but less stable than carbon monoxide. Some of these metals and metal complexes would likely work better than others however. For example, elemental zinc is a gas in the specified temperature range, so once it is reduced by carbon, it would join the gas phase and require complicated separation downstream. Indium is a rare and expensive metal, so implementation would not be economical. Iron titanium oxide and cerium oxide have both been studied for this exact purpose as well, so they do not demand further

justification for research. At these temperatures, elemental iron is also likely to bond with free carbon molecules, forming cementite, which would not be desirable within the process.

This leaves a total of five possible metals worthwhile for further experimental investigation which can be seen in Table 1.

Table 1: Five likely materials for high purity methane to syngas conversion.

Compound Name	Composition	Melting Point (°C) [FactSage]
Fayalite	Fe_2SiO_4	1205
Ferberite	$FeWO_4$	> 1800
Cobalt Chromate (spinel)	$CoCr_2O_4$	> 1800
Beryllium Tungstate	$BeWO_4$	> 1800
Niobium Pentoxide	Nb_2O_5	1512

Of particular interest in this investigation is fayalite since this material is conceptually similar to iron titanium oxide, however silicon is a far cheaper alternative to titanium to serve as an iron backbone, and only half as much Fe_2SiO_4 would be required when compared to $FeTiO_3$ for the same oxidative capability. This means that less energy would have to be expended on heating the materials in the methane oxidation reactor which still requires temperatures above 700°C to operate properly. A simple investigation in to the kinetics and syngas compositions produced by these materials is therefore recommended in order to determine their practical applicability. If these materials work as theorized, then they could serve as the foundation for more advanced materials which could be used industrially to make syngas more efficiently. Higher purity syngas is beneficial since it reduces or eliminates the need for downstream processes to remove carbon dioxide from the syngas.

An example of a methane reforming process using chemical looping fundamentals is shown below in Figure 18 using fayalite as an example material. Thermodynamic verification of this process can be found in Appendix G.

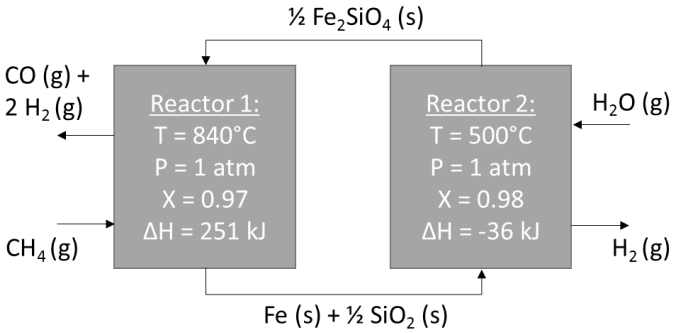

Figure 18: Simple chemical looping system to produce syngas from methane using fayalite.

This system has some significant benefits. First, high purity syngas is thermodynamically predicted. Additionally, the reduction of water to produce additional hydrogen can be performed at similar temperatures, reducing the temperature swing between the two reactors. Even at 840°C, with no temperature or pressure swing, a conversion of 88% can be achieved in reactor 2. The reduced metal complex could also be oxidized in air, rather than water, which would be significantly more exothermic (ΔH = -277 kJ at 840°C) and could be used to heat the first reactor. This system therefore has high potential for industrial implementation if the reaction kinetics and thermodynamics can be verified experimentally.

Conclusions

Seven chemical looping reaction pathways were presented and justified for the purpose of cleaner fuel generation. Their significance and practicality vary, however they are universally thermodynamically sound. A broad recommendation for future work regarding all of the developed cycles would be to experimentally analyze the proposed reaction pathways in order to determine their actual kinetics and thermodynamics. Economic and system energy analyses should also be performed in order to determine the industrial practicality of these cycles.

Aluminum cerium oxide was used to produce a two-reactor STWS cycle which reduced water to hydrogen at low temperatures around 260°C, and the metal complex was reduced around 1600°C. This system had a very high overall conversion, above 99%, and could be further optimized using modeling software like Aspen. Aluminum cerium oxide is a relatively inexpensive material, and solar thermal energy would be used to heat the two reactors. The only continuous inputs to the system once constructed would be solar thermal heat and water, both of which are highly abundant. The main issue with this cycle is the reducer temperature, 1600°C, which is still too high for practical solar thermal heating. This temperature could be further reduced by lowering the partial pressure of oxygen in the reducer or by destabilizing the lattice structure of the aluminum cerium oxide by doping it with additional metals. If the temperature in the reducer could be lowered to below 1200°C, then solar thermal energy would likely be sufficient for supplying all of the heat required for the aluminum cerium oxide auto-thermal reduction. If this were achieved and the reaction rates were fast enough then this cycle could likely find significant industrial applications due to its overall simplicity.

Another way to reduce the high temperature required for aluminum cerium oxide reduction is to react it with elemental sulphur at temperatures around 1000°C. At this temperature, the metal complex is reduced and sulphur dioxide is produced. It is theorized that this sulphur dioxide could then be electrically separated back in to its constituent components using electrolysis. This would require only about two-thirds of the electricity required to directly perform electrolysis on water. There are some large concerns with this process however. Primarily, it would need to occur above the melting point of sulphur in order to prevent the electrode from being coated in solid sulphur, at this temperature sulphur dioxide is a gas though and gas-phase electrolysis has complications. Before experimental analysis is required, an overall energy balance should be performed on the system to determine if the combination of heating and pumping the aluminum cerium oxide, in addition to the electrolysis of sulphur dioxide, is less energy intensive than pure electrolysis of water.

There is a very common industrial process though in which sulphur is oxidized in air to sulphur dioxide in order to produce sulphuric acid, known as the contact process. Rather than oxidation in air, the sulphur could be oxidized by aluminum cerium oxide in order to be more efficient; this reduced aluminum cerium oxide could then be used as previously proposed, to split water in to hydrogen in a separate reactor. The sulphur dioxide produced could then be used to make sulphuric acid. This process only requires moderate modifications to existing industrial processes, so it could be implemented rather cheaply as an entirely new system would not need to be purchased. The hydrogen produced could then be sold as a fuel. With an input of both carbon dioxide and water, rather than solely water, this process could theoretically be used to produce methane alongside of sulphuric acid. The methane could be sold or further reformed in to syngas. This process could utilize environmental carbon dioxide, and as a result

would be a carbon-negative system. This would be a far more environmentally friendly way to produce methane versus the current standard of hydraulic fracturing which has many environmental concerns surrounding it. As a result of being carbon-negative, carbon credits could also be sold to other companies if applicable.

Another possibility for producing hydrogen from water is to use the sulphur-iodine cycle, an old proposition by General Atomics which never reached industrial fruition. This was due to a couple of large concerns revolving around the feasibility of the process. Rather than heating the sulphuric acid directly to very high temperatures, it can be reduced via palladium at more moderate temperatures. The palladium oxide produced can then be auto-thermally reduced in a separate reactor, eliminating the need to heat sulphuric acid to nearly 900°C, and removing the need for the advanced materials required to hold sulphuric acid at that temperature. The original sulphur-iodine cycle also suffered from low conversions of hydroiodic acid decomposition. This was enhanced by using hydrobromic acid instead of hydroiodic acid, and reacting it with silver to form silver bromide, a highly photosensitive material which will decompose under ultraviolet radiation. This further removes the need for high temperatures to decompose the hydrobromic acid. Kinetic data on the photodecomposition of silver bromide could not be found in literature, and consequently, this step of the process is highly uncertain. Experimental analysis is therefore necessary to determine if this process is practical or even possible. If it is kinetically practical, this cycle stands to be highly implementable industrially for the same reasons that the sulphur-iodine cycle: it operates at a relatively low temperature for STWS and most of the materials are either gases or liquids, making them easily transportable. This system is more complicated than the aluminum cerium oxide STWS cycle though as it has five separate reactors and would require a larger initial investment.

Hydrogen production from methane was also a focus for investigation. Most methane reforming processes operate a temperatures above 700°C in order to achieve higher carbon monoxide concentrations, however the carbon monoxide is commonly further oxidized with water to produce more hydrogen in addition to carbon dioxide. If the aim is to produce hydrogen and carbon dioxide though, a lower temperature option exists. Cadmium hydroxide can be produced by reacting elemental cadmium with water, resulting in the production of hydrogen at low temperatures. The cadmium hydroxide can then be reduced back to elemental cadmium by reacting it with methane at 400°C, producing water and carbon dioxide. The water is then recycled to react with the elemental cadmium. In this way, hydrogen can be efficiently produced from methane at temperatures over 300°C below the current industrial standard. For obvious reasons, this reduces the amount of energy required to operate the system, and because of the high conversions for both reactions, downstream separation equipment is less necessary. If the goal was to produce syngas rather than just hydrogen, then the carbon dioxide produced could be reacted with either water or methane in order to produce a syngas mixture. Due to thermodynamic constraints, this reaction would need to take place at higher temperatures in order to partially reduce the carbon dioxide.

Materials were also investigated for use in current methane reforming systems which allowed for a higher carbon monoxide selectivity. These materials fall within the free energy gap between carbon monoxide and carbon dioxide at temperatures above 700°C. Of the materials discovered, some were deemed less desirable as a result of likely side reactions or complicated separation issues. Five new metal oxides were found which should act theoretically similar to iron titanium oxide, a material that has been shown to increase syngas purity. Of these materials, fayalite, Fe_2SiO_4, stood out as being particularly

advantageous because of its similarity to iron titanium oxide, but also because it is cheaper than iron titanium oxide and less of it is required for the same oxidative capabilities.

All of these systems have very practical possibilities for industrial implementation if the experimental analysis is similar to the thermodynamic analysis. It is therefore recommended that these cycles be experimentally investigated in order to determine their actual thermodynamic and kinetic capabilities. Those reaction pathways which appear experimentally sound should then be simulated and economically analyzed to determine if they are industrially viable, and those which are found to be industrially viable have a large potential to impact the production of hydrogen and syngas in a more efficient and sustainable way.

Bibliography

1. "U.S. Energy Information Administration - EIA - Independent Statistics and Analysis." *International Energy Outlook 2016-World energy demand and economic outlook - Energy Information Administration*. N.p., 11 May 2016. Web. DOE/EIA-0484 (2016)
2. "Future of Climate Change." *EPA*. Environmental Protection Agency, 27 Dec. 2016. Web.
3. Yilmaz, F., Balta, M. T. & Selbaş, R. *A review of solar based hydrogen production methods*. *Renew. Sustainable Energy Rev.* 56, 171–178 (2016).
4. WIREs Energy Environ 2016, 5:261–287. doi: 10.1002/wene.174
5. "Hydrogen Production: Natural Gas Reforming." *Hydrogen Production: Natural Gas Reforming | Department of Energy*. N.p., n.d. Web.
6. Mackaluso, Joshua D. "The Use of Syngas Derived From Biomass and Waste Products to Produce Ethanol and Hydrogen." *Microbiology and Molecular Genetics* 445 (2007): 98-103. Web.
7. Bonaquist, Dante. *Analysis of CO2 Emissions, Reductions, and Capture for Large-Scale Hydrogen Plants*. Rep. N.p.: n.p., October 2010. *PRAXAIR*. Web.
8. http://www.making-hydrogen.com/steam-reforming-hydrogen.html
9. "Production: Growth In Most Regions." *Chemical and Engineering News* (n.d.): n. pag. American Chemical Society, 11 July 2005. Web. <http://pubs.acs.org/cen/coverstory/83/pdf/8328production.pdf>.
10. "Global Sulfuric Acid Production Surpassed 230.7 Million Tonnes in 2012." | Merchant Research & Consulting, Ltd., 6 Sept. 2016. Web.
11. United States. Department of Energy. *Report of the Hydrogen Production Expert Panel: A Subcommittee of the Hydrogen & Fuel Cell Technical Advisory Committee*. N.p., May 2013. Web.
12. http://www.meritnation.com/ask-answer/question/can-u-show-a-bigger-picture-of-the-contact-process-for-more/chemistry/2792575
13. Besenbruch, G. 1982. General Atomic sulfur iodine thermochemical water-splitting process. Proceedings of the American Chemical Society, Div. Pet. Chem., 27(1):48-53.
14. Sau, Salvatore, et.al. “Decrease the rate of recycling agents in the sulphur-iodine cycle by solid phase separation”. *International Journal of Hydrogen Energy,* 2008, 33(22): 6439-6444.
15. Cady, H. P., and Robert Taft. "Electrolysis in Liquid Sulphur Dioxide." *The Journal of Physical Chemistry* (1924): 1075-084. Print. DOI: 10.1021/j150255a004
16. Sarker, Nilay Kumar, and Tanveer Ahmed Khan. "Simulation of the Production of Sulfuric Acid from a Sulfur-burning Single-absorption Contact Sulfuric Acid Plant." *Journal of Emerging Technologies and Innovative Research* 2.6 (June 2015): 2006-011. Web. JETIR (ISSN-2349-5162)
17. Müller, H. 2000. Sulfur Dioxide. Ullmann's Encyclopedia of Industrial Chemistry.
18. Kubo, Shinji, et.al. “R&D Program on Themochemical Water-Splitting Iodine-Sulphur Process at JAERI.” Department of Advanced Nuclear Heat Technology, Japan Atomic Energy Research Institute. Sep., 2003. Web.
19. Scott, A. (1900). "Preparation of Pure Hydrobromic Acid". *Journal of the Chemical Society, Transactions*. 77: 648–651.
20. Greenwood, N.N., Earnshaw, A. (1984). *Chemistry of the Elements*. New York: Permagon Press. pp. 1185–87. ISBN 0-08-022057-6.
21. Sowerby (ed.), A.L.M. (1961), *Dictionary of Photography: A Reference Book for Amateur and Professional Photographers* (19th ed.), London: Illife Books Ltd.

22. Burley, G. 1963. “Photolytic Behavior of Silver Iodide.” *Journal of Research of the National Bureau of Standards* Vol.67A, No.4 (1963): 301-307. Web. NIST.
23. Guo, H.F., P. Zhang, Y. Bai, L.J. Wang, S.Z. Chen, and J.M. Xu (3 June 2009). "Continuous purification of H2SO4 and HI phases by packed column in IS process". *International Journal of Hydrogen Energy*. Elsevier Ltd. 35 (7): 2837.
24. Luo, Siwei, Zeng, Liang, et.al. “Shale gas-to-syngas chemical looping process for stable shale gas conversion to high purity syngas with a H_2 : CO ratio of 2 : 1.” *Energy Environmental Science,* 2014, 7: 4104-4117.

A: Aluminum Cerium Oxide: Two-Reactor Solar Thermal Water Splitting

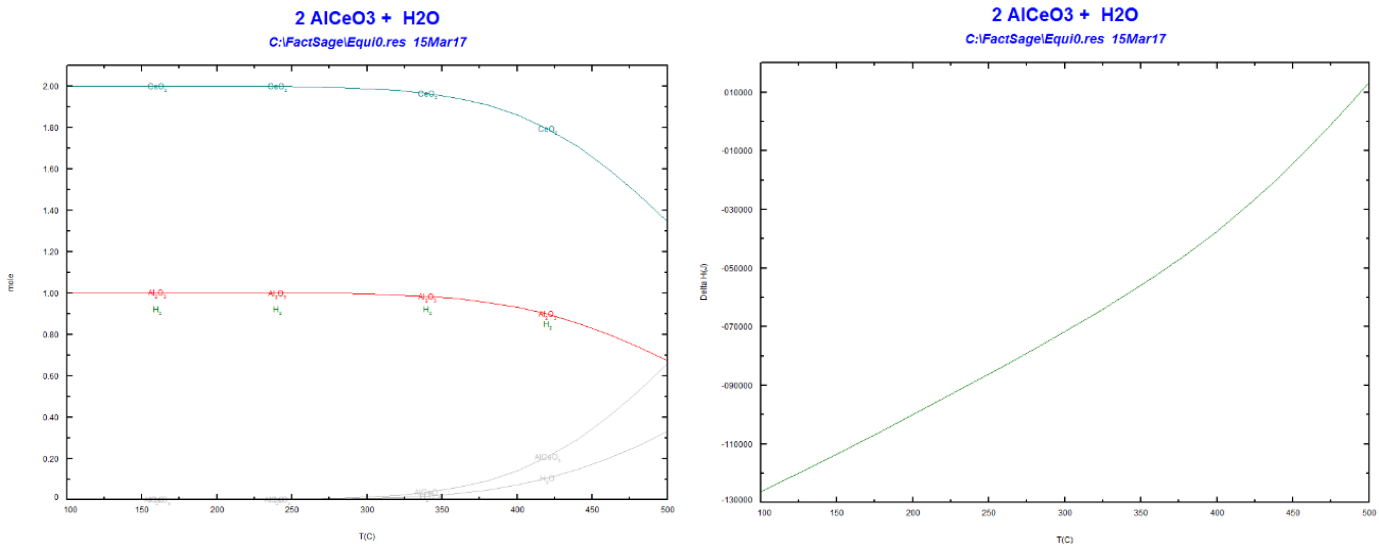

Figure 19: Composition and enthalpy as a function of temperature in Reactor 1. Initial reactants are shown at the top of the graphs. Initial conditions: T = 200°C, P = 1 atm

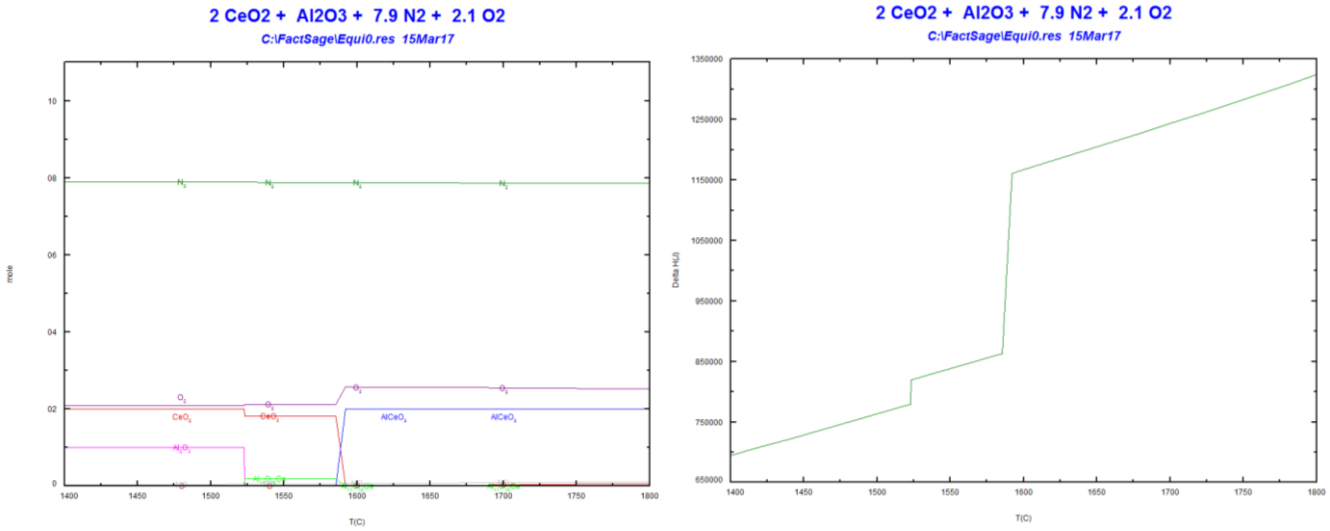

Figure 20: Composition and enthalpy as a function of temperature in Reactor 2. Initial reactants are shown at the top of the graphs. Initial conditions: T = 1080°C, P = 0.5 atm

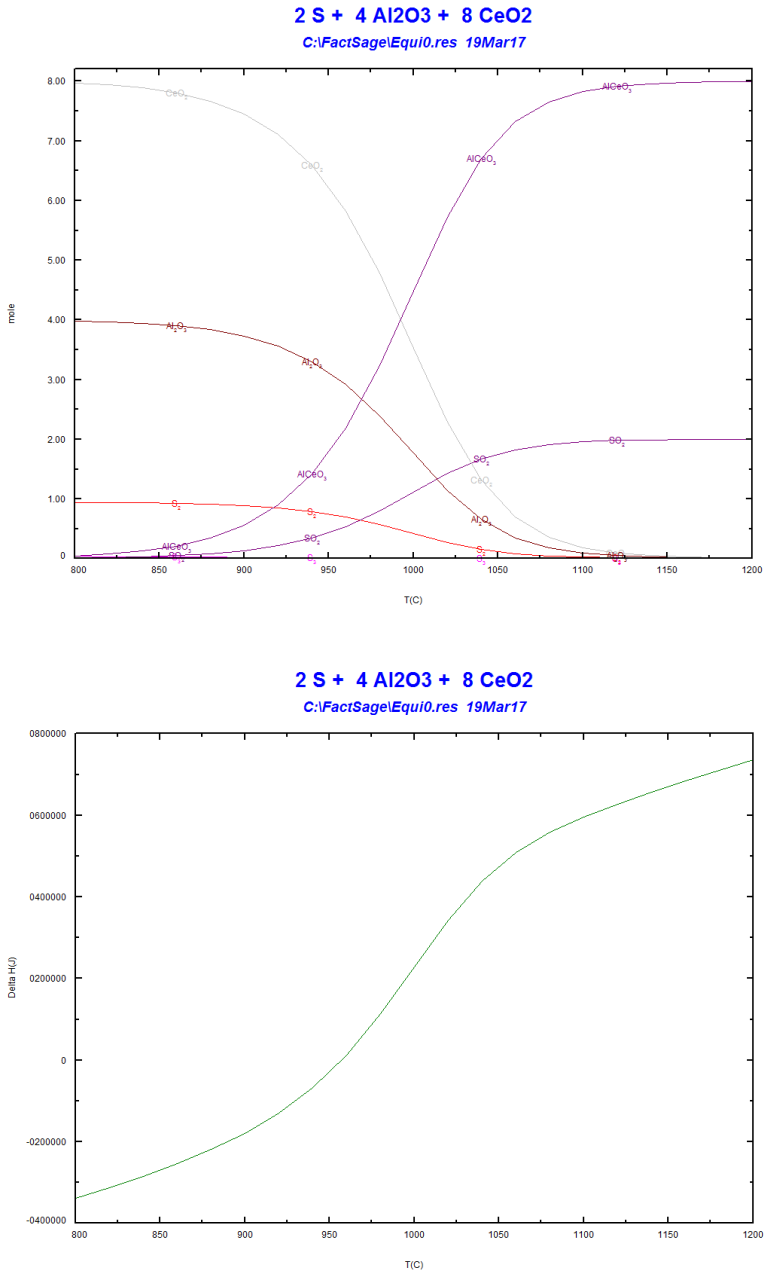

Figure 21: Composition (top) and enthalpy (bottom) as a function of temperature in Reactor 2. Initial reactants are shown at the top of the graphs.
Initial conditions: T = 1080°C, P =0.5 atm

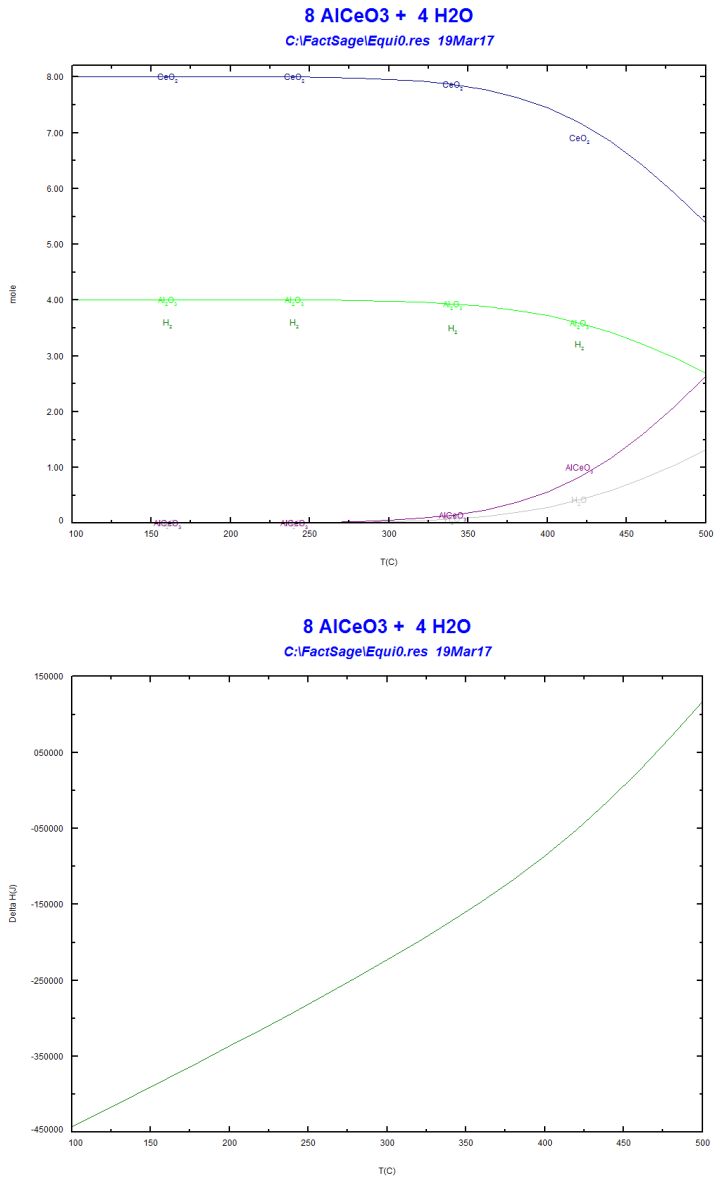

Figure 22: Composition (top) and enthalpy (bottom) as a function of temperature in Reactor 1. Initial reactants are shown at the top of the graphs. Initial conditions: T = 200°C, P = 1 atm

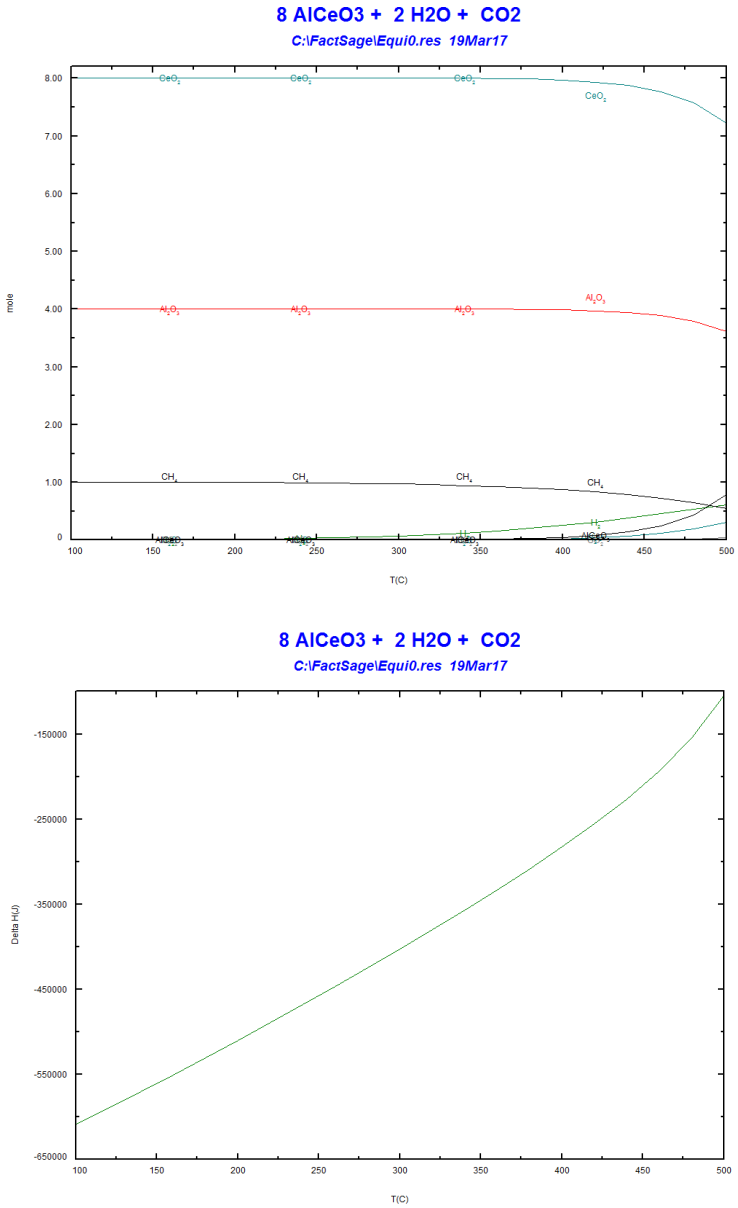

Figure 23: Composition (top) and enthalpy (bottom) as a function of temperature in Reactor 1. Initial reactants are shown at the top of the graphs. Initial conditions: T = 200°C, P = 1 atm

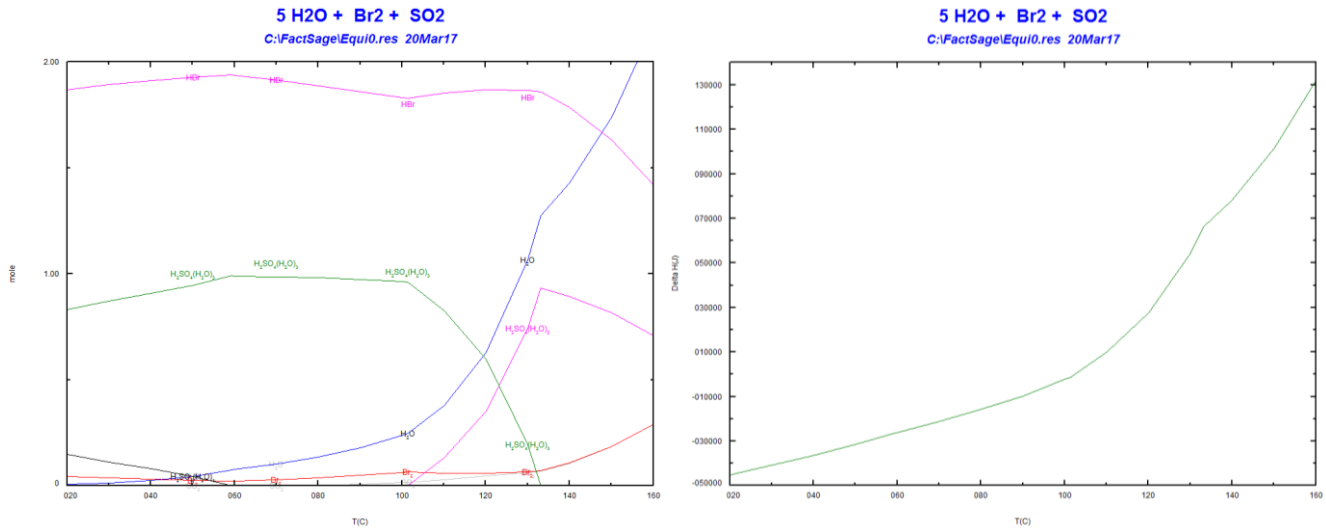

Figure 24: Composition and enthalpy as a function of temperature in Reactor 1. Initial reactants are shown at the top of the graphs. Initial conditions: T = 60°C, P = 1 atm

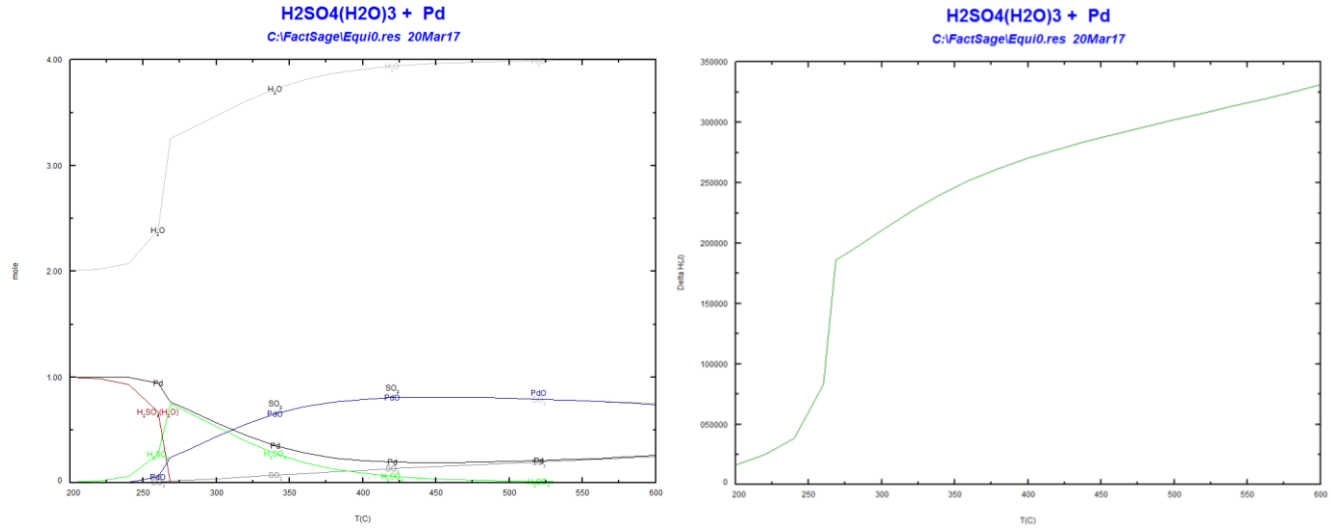

Figure 25: Composition and enthalpy as a function of temperature in Reactor 2. Initial reactants are shown at the top of the graphs. Initial conditions: T = 400°C, P = 1 atm

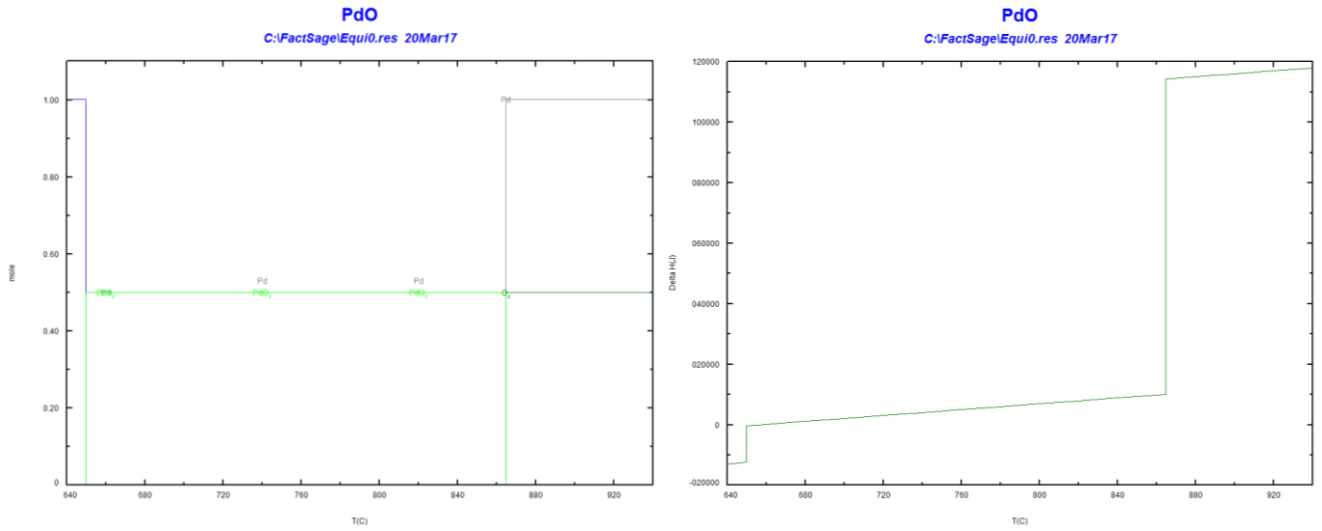

Figure 26: Composition and enthalpy as a function of temperature in Reactor 3. Initial reactants are shown at the top of the graphs. Initial conditions: T = 870°C, P = 1 atm

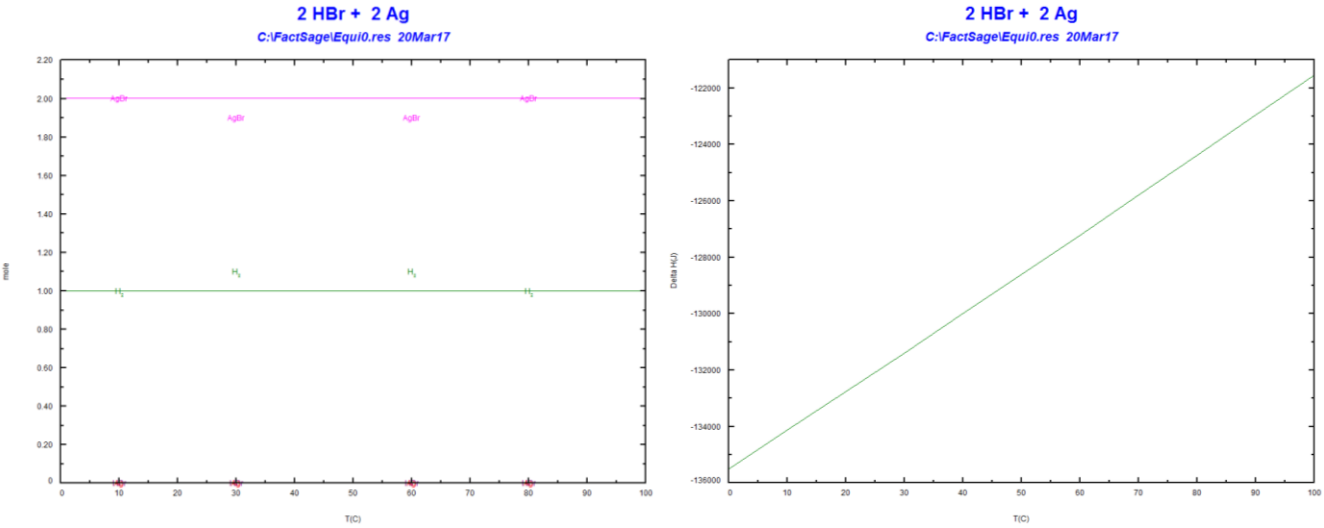

Figure 27: Composition and enthalpy as a function of temperature in Reactor 4. Initial reactants are shown at the top of the graphs. Initial conditions: T = 60°C, P = 1 atm

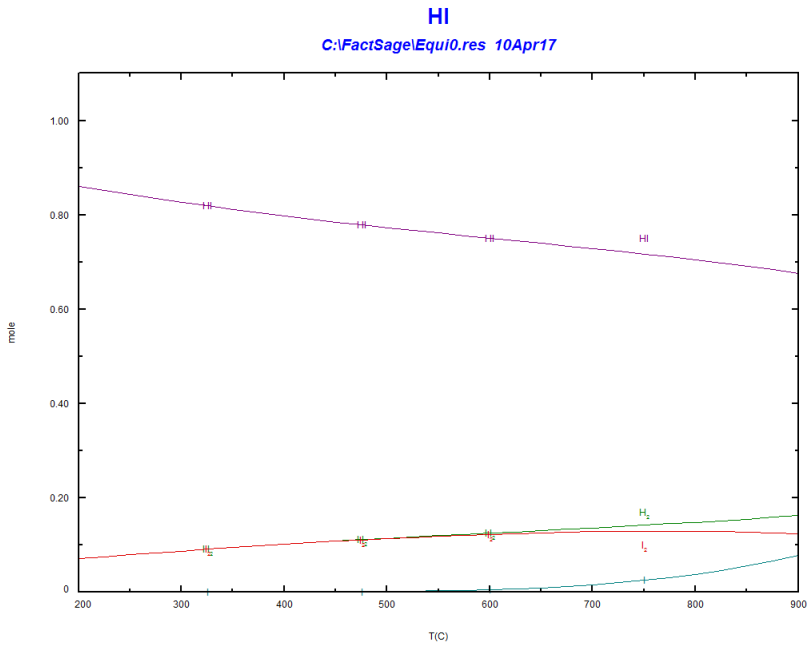

Figure 28: Thermal decomposition of HI to its components from 200-900°C.

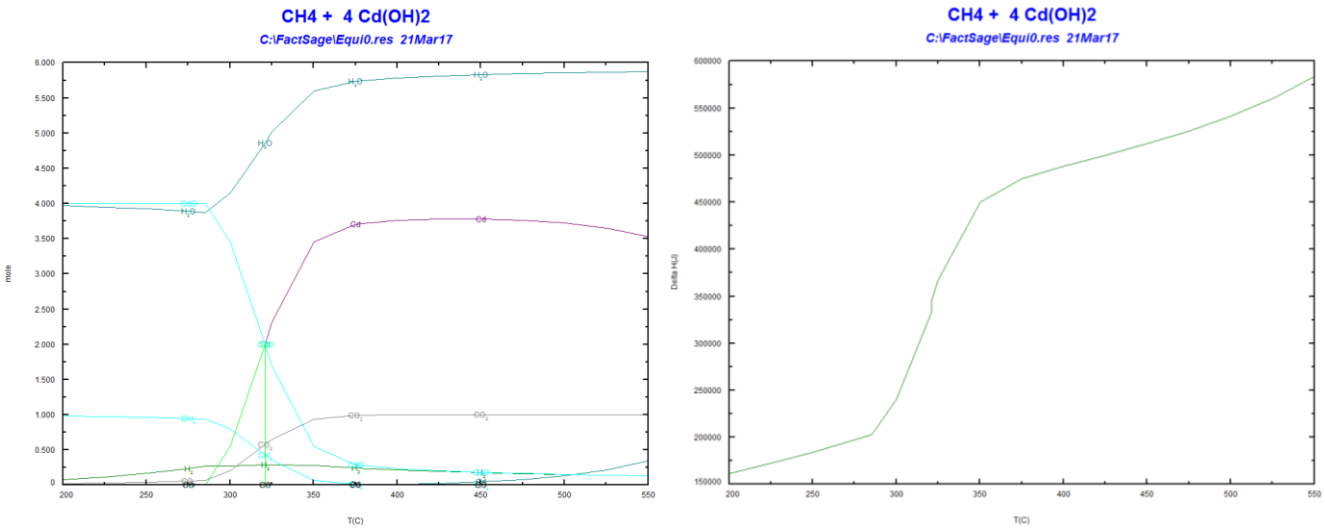

Figure 29: Composition and enthalpy as a function of temperature in Reactor 1. Initial reactants are shown at the top of the graphs. Initial conditions: T = 400°C, P = 1 atm

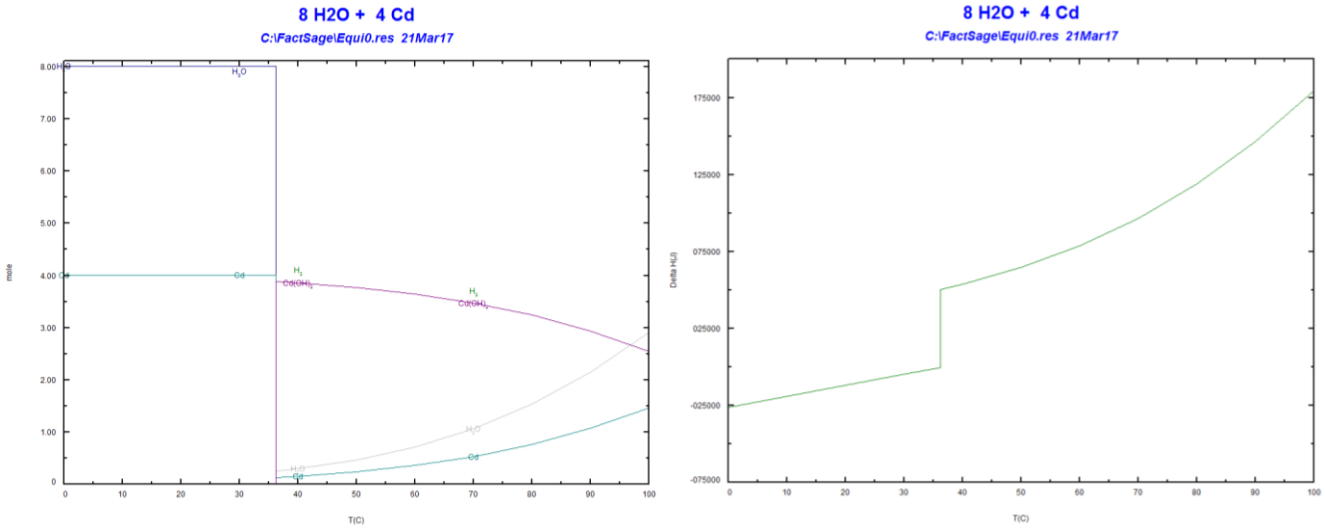

Figure 30: Composition and enthalpy as a function of temperature in Reactor 2. Initial reactants are shown at the top of the graphs. Initial conditions: T = 37°C, P = 1 atm

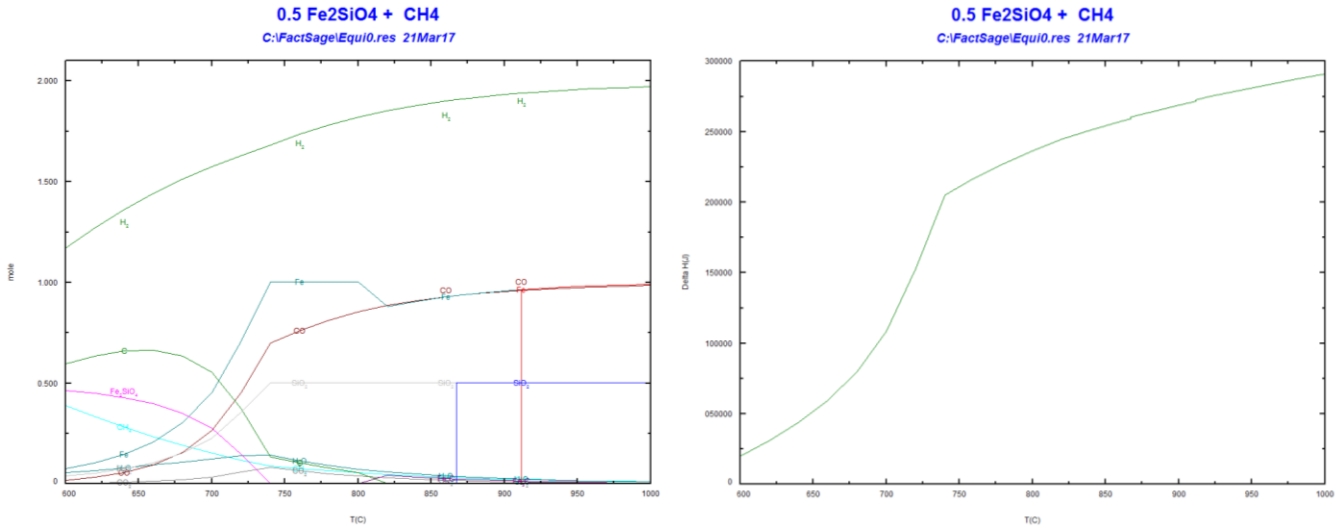

Figure 31: Composition and enthalpy as a function of temperature in Reactor 1. Initial reactants are shown at the top of the graphs. Initial conditions: T = 840°C, P = 1 atm

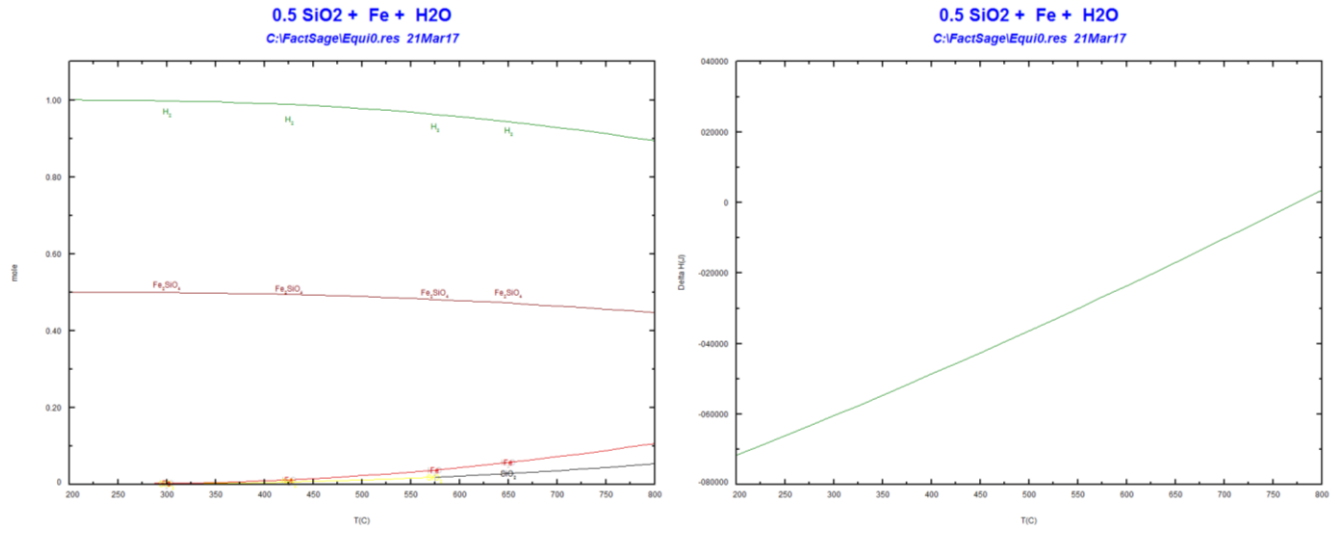

Figure 32: Composition and enthalpy as a function of temperature in Reactor 2. Initial reactants are shown at the top of the graphs. Initial conditions: T = 500°C, P = 1 atm

H: Thermodynamic Data for Modified Ellingham Diagram

The tables below contain the thermodynamic data used to create Figure 6, the modified Ellingham Diagram.

Fe + 0.5 O2 = 1/3 Fe + 1/3 Fe2O3		Fe + 0.5 O2 = FeO		Cu + 0.5 O2 = CuO		Ni + 0.5 O2 = NiO		2 AlCeO3 + 0.5 O2 = 2 CeO2 + Al2O3		1/3 FeTi + 0.5 O2 = 1/3 FeTiO3	
T	ΔG	T	ΔG	T	ΔG	T	ΔG	T	ΔG	T	ΔG
300	-247823.6	300	-244742	300	-128136	300	-211571	300	-281902	300	-372059.1
350	-243270.8	350	-241272	350	-123499	350	-206814	350	-274208	350	-367625.7
400	-238761.5	400	-237882	400	-118897	400	-202110	400	-266512.9	400	-363224.5
450	-234298.4	450	-234563	450	-114336	450	-197471	450	-258826.1	450	-358858.5
500	-229880.4	500	-231302	500	-109814	500	-192910	500	-251154	500	-354527.9
550	-225505	550	-228088	550	-105331	550	-188431	550	-243499.8	550	-350231.5
600	-221169.6	600	-224910	600	-100886	600	-183989	600	-235865.3	600	-345967.4
650	-216871.5	650	-221761	650	-96474.9	650	-179559	650	-228250.7	650	-341733.5
700	-212608.1	700	-218630	700	-92097.4	700	-175150	700	-220655.8	700	-337527.6
750	-208377.7	750	-215512	750	-87751.2	750	-170766	750	-213079.4	750	-333347.6
800	-204178.8	800	-212399	800	-83434.8	800	-166408	800	-205520.3	800	-329191.4
850	-200010.6	850	-209285	850	-79146.6	850	-162075	850	-197977.2	850	-325057.3
900	-195873.4	900	-206162	900	-74884.9	900	-157763	900	-190448.3	900	-320943.5
950	-191769.1	950	-203023	950	-70648.6	950	-153472	950	-182932.2	950	-316848.4
1000	-187686.6	1000	-199859	1000	-66436.3	1000	-149200	1000	-175427.2	1000	-312770.5
1050	-183596	1050	-196659	1050	-62246.7	1050	-144944	1050	-167931.8	1050	-308708.6
1100	-179495.9	1100	-193431	1100	-58078.8	1100	-140705	1100	-160444.4	1100	-304661.4
1150	-175394.7	1150	-190193	1150	-53931.5	1150	-136479	1150	-152963.4	1150	-300627.6
1184.81	-172540.1	1184.81	-187936	1200	-49803.6	1200	-132266	1200	-145487.5	1200	-296606.3
1184.81	-172540.1	1184.81	-187936	1250	-45693.7	1250	-128065	1250	-138015.1	1250	-292596.5
1200	-171287.2	1200	-186939	1300	-41600.2	1300	-123875	1300	-130545	1300	-288597.3
1250	-167170	1250	-183669					1300	-130545		
1300	-163063.8	1300	-180416					1350	-123075.2		

C + 0.5 O2 = CO, P = 0.1 atm		Fe + TiO2 + 0.5 O2 = FeTiO3		CrCeO3 + 0.5 O2 = CeO2 + CrO2		0.4 NiSb + 0.5 O2 = 0.4 NiO + 0.2 Sb2O3		MnO + 0.5 O2 = MnO2	
T	ΔG	T	ΔG	T	ΔG	T	ΔG	T	ΔG
300	-140183.7	300	-266902.9	300	-103133	300	-177577.5	300	-100610
350	-145149.4	350	-263346.8	350	-98491	350	-172752.5	350	-95148
400	-150145.1	400	-259838.5	400	-93984.3	400	-167982.4	400	-89668.9
450	-155156.4	450	-256375.8	450	-89626.8	450	-163272.6	450	-84190.5
500	-160173.1	500	-252954.5	500	-85421.6	500	-158628.5	500	-78724.2
550	-165188.1	550	-249569.3	550	-81363.8	550	-154053.7	550	-73277.7
600	-170196.6	600	-246214.9	600	-77446.8	600	-149531.7	600	-67856
650	-175195.1	650	-242885.6	650	-73663.3	650	-145055.6	650	-62462.3
700	-180181.5	700	-239575.7	700	-70004.5	700	-140622.3	700	-57098.7
750	-185154.2	750	-236279.4	750	-66461.9	750	-136229.6	750	-51766.5
800	-190112.4	800	-232990.8	800	-63027.8	800	-131875.9	800	-46466.3
850	-195055.6	850	-229703.5	850	-59695.1	850	-127559.8	850	-41198.5
900	-199983.6	900	-226410.7	900	-56457.2	879	-125073.4	900	-35962.9
950	-204896.4	950	-223104.6	950	-53307.8	879	-125073.4	950	-30759.4
1000	-209794.2	1000	-219776.1	1000	-50241.7	900	-123310.8	1000	-25587.5
1050	-214677.4	1050	-216413.8	1050	-47253.8	928	-120965.6	1050	-20446.9
1100	-219546.1	1100	-213023.7	1100	-44339.9	928	-120965.6	1100	-15337
1150	-224400.7	1150	-209622.9	1150	-41495.8	950	-119389.5	1150	-10257
1200	-229241.5	1184.81	-207252.8	1200	-38717.9	1000	-115832.8	1200	-5206.4
1250	-234068.9	1184.81	-207252.8	1250	-36003.2	1050	-112309.6	1250	-184.5
1300	-238883.2	1200	-206206.6	1300	-33350.5	1100	-108817.4	1300	4809.5
		1250	-202771.9			1150	-105354.4		
		1300	-199351.6			1200	-101918.8		
						1250	-98509.1		
						1300	-95123.8		

3 CoO + 0.5 O2 = Co3O4		0.5 V2O3 + 0.5 O2 = 0.5 V2O5		Ce6O11 + 0.5 O2 = 6 CeO2		Cr2O3 + 0.5 O2 = 2 CrO2		MoO2 + 0.5 O2 = MoO3		2/3 Bi + 0.5 O2 = 1/3 Bi2O3	
T	ΔG	T	ΔG	T	ΔG	T	ΔG	T	ΔG	T	ΔG
300	-152651.1	300	-140012.1	300	-298357.6	300	-10472.4	300	-135952.7	300	-165528.8
350	-145075.9	350	-135693.4	350	-291599.2	350	-6501.8	350	-132410.8	350	-161034.7
400	-137192.4	400	-131375.6	400	-284846.7	400	-3059	400	-128901.7	400	-156585.4
450	-129087.7	450	-127067.6	450	-278104.8	450	-77.5	450	-125420.7	450	-152174.7
500	-120817.5	500	-122774.3	500	-271374.6	500	2497.3	500	-121963.9	500	-147796.9
550	-112422.6	550	-118498.3	550	-264655.4	550	4708.1	550	-118528.5	544	-143967.9
600	-103935	600	-114240.5	600	-257945.6	600	6588.6	600	-115112.9	544	-143967.9
650	-95381.8	650	-110001.5	650	-251243.8	650	8166.8	650	-111716.4	550	-143364.2
700	-86786.1	700	-105781	700	-244548	700	9470.1	700	-108338.8	600	-138346.6
750	-78168.2	750	-101578.6	750	-237856.8	750	10522.7	750	-104980.5	650	-133354
800	-69546.3	800	-97393.7	800	-231168.6	800	11345	800	-101642.2	700	-128387.9
850	-60936.2	850	-93225.7	850	-224481.9	850	11954.5	850	-98324.8	750	-123449.2
900	-52352.6	900	-89073.9	900	-217795.5	900	12366.5	900	-95029.3	800	-118538.8
950	-43808.3	943	-85515.6	950	-211108.4	950	12594.4	950	-91756.8	850	-113657.2
1000	-35315.1	943	-85515.6	1000	-204419.3	1000	12649.9	1000	-88508.6	900	-108804.7
1050	-26883.5	950	-85176.9	1050	-197727.6	1050	12543.5	1050	-85285.7	950	-103981.7
1100	-18522.9	1000	-82772.2	1100	-191032.2	1100	12284.8	1074	-83748.1	1000	-99188.5
1150	-10242.1	1050	-80390.1	1150	-184332.4	1150	11882.1	1074	-83748.1	1003	-98901.8
1200	-2048.6	1100	-78027.4	1200	-177627.6	1200	11343.1	1100	-83268.8	1003	-98901.8
1250	6050.4	1150	-75681.5	1250	-170919	1250	10675	1150	-82390	1050	-94892.7
1300	14048.6	1200	-73349.9	1300	-164215.9	1300	9884	1200	-81563.4	1098	-90828.9
		1250	-71030					1250	-80783.9	1098	-90828.9
		1300	-68719.9					1300	-80046.9	1100	-90669.2
										1150	-86712.7
										1200	-82824.6
										1250	-79001.8
										1300	-75241.5

0.5 FeV2O4 + 0.5 O2 = 0.5 FeV2O6		0.5 S + 0.5 O2 = 0.5 SO2		MnTiO3 + 0.5 O2 = MnO2 + TiO2		Ba + TiO2 + 0.5 O2 = BaTiO3		NaNO2 + 0.5 O2 = NaNO3		Co + TiO2 + 0.5 O2 = CoTiO3	
T	ΔG	T	ΔG	T	ΔG	T	ΔG	T	ΔG	T	ΔG
300	-171143.4	300	-150072.3	300	-68910.6	300	-682781.2	300	-80840.8	300	-239896.1
350	-166831.9	350	-150321.8	350	-63759.7	350	-677427.3	303.99	-80514.1	350	-235653
400	-162571.3	368.3	-150402.1	400	-58585.2	394.65	-672683.8	303.99	-80514.1	400	-231500.4
450	-158354.7	368.3	-150402.1	450	-53403.9	394.65	-672683.8	350	-76365.7	450	-227423.4
500	-154176.3	388.36	-150472.9	500	-48228.8	400	-672120.5	400	-71834.5	500	-223409.3
550	-150030.8	388.36	-150472.9	550	-43068.9	450	-666865.5	434	-68736.2	550	-219447.8
600	-145914.1	400	-150484.7	600	-37930.6	500	-661616	434	-68736.2	600	-215530.2
650	-141822.5	450	-150493.7	650	-32818.3	550	-656346.6	450	-67185.7	650	-211649.8
700	-137753.1	500	-150433.7	700	-27734.9	600	-651037.9	500	-62272.8	694.99	-208185.2
750	-133703.3	550	-150317.2	750	-22682.3	650	-645736	550	-57307.1	694.99	-208185.2
800	-129670.9	600	-150155.6	800	-17661.6	700	-640442.8	550	-57307.1	700	-207797.7
850	-125654	650	-149957.3	850	-12673.6	750	-635143.1	550	-57307.1	750	-203944.2
900	-121651.2	700	-149728	900	-7718.2	800	-629829.8	557	-56667.1	800	-200112.7
950	-117661.4	750	-149471.8	950	-2795.7	850	-624519.7	557	-56667.1	850	-196299.5
1000	-113683.4	800	-149192.2	1000	2094.5	900	-619214.5	583	-53616.1	900	-192501
1050	-109716	850	-148892.2	1050	6952.5	950	-613914.1	583	-53616.1	950	-188713.9
1100	-105757.2	900	-148573.4	1100	11779.1	1000	-608618.7	600	-52088.7	1000	-184935.4
1150	-101804.8	950	-148237.4	1150	16574.7	1000	-608618.7	650	-47705.3	1050	-181162.3
1200	-97856.5	1000	-147885.1	1200	21340.2	1000	-608618.7	700	-43474.1	1100	-177391.7
1250	-93910.4	1050	-147517.9	1250	26076.1	1050	-602922.8	750	-39383.6	1150	-173620.5
1300	-89964.6	1100	-147136.4	1300	30783.3	1100	-597223.6	800	-35423.5	1200	-169845.5
		1150	-146741.5			1150	-591523.1	850	-31585.3	1250	-166063.3
		1200	-146334			1200	-585823	900	-27861.2	1300	-162269.7
		1250	-145914.4			1250	-580124.8	950	-24244.5		
		1300	-145483.4			1300	-574429.8	1000	-20729.1		
								1050	-17309.7		
								1100	-13981.5		
								1150	-10740		
								1200	-7581.3		
								1250	-4501.7		
								1300	-1497.9		

SO2 + 0.5 O2 = SO3		0.25 (P2O3)2 + 0.5 O2 = 0.5 P2O5		2/3 B + 0.5 O2 = 1/3 B2O3		0.5 Se + 0.5 O2 = 0.5 SeO2		0.5 SiO2 + Fe + 0.5 O2 = 0.5 Fe2SiO4		0.5 Pd + 0.5 O2 = 0.5 PdO2	
T	ΔG	T	ΔG	T	ΔG	T	ΔG	T	ΔG	T	ΔG
300	-73151.9	300	-6907.3	300	-397011	300	-85584.6	300	-263100.2	300	-76920.9
317.19	-69116.8	350	-6632.8	350	-392584.8	350	-81079.7	350	-259367.5	350	-72324.3
317.19	-69116.8	400	-6370.5	400	-388155.7	400	-76599.3	400	-255675	400	-67727.8
350	-66022.4	450	-6115.3	450	-383729.1	450	-72148.8	450	-252021.9	450	-63131.4
400	-61294.7	500	-5864	500	-379308.6	494.3	-68233.1	500	-248404.7	500	-58535.3
450	-56561.6	550	-5615.1	550	-374896.8	494.3	-68233.1	550	-244818.5	550	-53939.9
500	-51829.1	600	-5367.7	600	-370495.4	500	-67697.3	600	-241257.9	600	-49345.2
550	-47101.3	650	-5121.9	650	-366105.7	550	-63007.2	650	-237716.7	650	-44751.4
600	-42380.6	700	-4877.8	700	-361728.7	597.39	-58581.7	700	-234188.1	700	-40158.6
650	-37668.7	750	-4635.6	723	-359719.8	597.39	-58581.7	750	-230664.7	750	-35567.1
700	-32966.7	800	-4395.6	723	-359719.8	600	-58575.8	800	-227138.7	800	-30976.7
750	-28275.1	850	-4157.8	750	-357668.2	650	-58449.3	848.01	-223742.6	850	-26387.7
800	-23594.2	900	-3922.6	800	-353897.5	700	-58296.4	848.01	-223742.6	900	-21800.2
850	-18924.3	950	-3690.1	850	-350160.4	750	-58120	850	-223600.7	950	-17214
900	-14265.2	1000	-3460.3	900	-346453.7	800	-57922.2	900	-220037.2	1000	-12629.5
950	-9616.8	1050	-3233.3	950	-342774.4	850	-57704.3	950	-216462.6	1050	-8046.5
1000	-4978.8	1100	-3009.1	1000	-339120.1	900	-57467.5	1000	-212867.9	1100	-3465
1050	-350.9	1150	-2787.6	1050	-335488.6	950	-57212.4	1050	-209242.3	1150	1114.8
1100	4267.1	1200	-2568.7	1100	-331878	1000	-56939.1	1100	-205591.8	1200	5693.2
1150	8875.5	1250	-2352.5	1150	-328286.7	1050	-56648	1140.09	-202659	1250	10270.2
1200	13474.6	1300	-2138.7	1200	-324713.2	1100	-56339.7	1140.09	-202659	1300	14846.1
1250	18064.7			1250	-321156.2	1150	-56015	1150	-201925.1		
1300	22646.2			1300	-317614.5	1200	-55674.5	1184.81	-199346		
						1250	-55318.8	1184.81	-199346		
						1300	-54948.4	1200	-198209.1		
								1250	-194477.5		
								1300	-190763.5		

2 Ag + 0.5 O2 = Ag2O		2 Rh + 0.5 O2 = Rh2O		Cd + 0.5 O2 = CdO		0.5 Ir + 0.5 O2 = 0.5 IrO2		0.5 Ru + 0.5 O2 = 0.5 RuO2		0.5 Re + 0.5 O2 = 0.5 ReO2		2 Fe3O4 + 0.5 O2 = 3 Fe2O3		Zn + 0.5 O2 = ZnO	
T	ΔG	T	ΔG	T	ΔG	T	ΔG	T	ΔG	T	ΔG	300	-203087.4	300	-320281
300	-11076.7	300	-79710.4	300	-229137	300	-94041	300	-126194.8	300	-195411	350	-196509.6	350	-315258
350	-7753.5	350	-77203.1	350	-224177	350	-89507.4	350	-121821.8	350	-190570.3	400	-189943.4	400	-310253.1
400	-4451.7	400	-74758.9	400	-219244	400	-85009.4	400	-117484.8	400	-185743.5	450	-183389.1	450	-305269.1
450	-1182.5	450	-72370.7	450	-214340	450	-80551.1	450	-113194	450	-180937.8	500	-176835.8	500	-300305.6
500	2047.2	500	-70032.3	500	-209461	500	-76133.1	500	-108953	500	-176156.5	550	-170265.7	550	-295360.7
550	5233.3	550	-67739.1	550	-204605	550	-71754.2	550	-104762.2	550	-171400.6	600	-163655.3	600	-290432.5
600	8373.3	600	-65487.1	594.22	-200328	600	-67412.7	600	-100620.8	600	-166670.2	650	-156975	650	-285518.6
650	11467.9	650	-63273.2	594.22	-200328	650	-63106.4	650	-96526.8	650	-161964.9	700	-150189.8	692.73	-281329
700	14522.4	700	-61094.6	600	-199709	700	-58833.1	700	-92478.2	700	-157283.8	750	-143259.9	692.73	-281329
750	17542.8	750	-58949.5	650	-194370	750	-54590.8	750	-88472.8	750	-152625.9	800	-136141.6	700	-280540.1
800	20534.2	800	-56835.9	700	-189048	800	-50377.4	800	-84508.5	800	-147990.4	848.12	-129071	750	-275117.1
850	23501.3	850	-54752.7	750	-183743	850	-46191	850	-80583	850	-143376.1	848.12	-129071	800	-269699.8
900	26448.2	900	-52698.5	800	-178454	900	-42030.2	900	-76694.5	900	-138782.2	850	-128782.8	850	-264288.7
950	29378.8	950	-50672.7	850	-173181	950	-37893.3	950	-72841.2	950	-134208	900	-121267.1	900	-258884.3
1000	32296.4	1000	-48674.3	900	-167923	1000	-33779	1000	-69021.7	1000	-129652.9	950	-114067.8	950	-253487.1
1050	35204.1	1050	-46701.1	950	-162681	1050	-29686	1050	-65234.5	1050	-125116.4	1000	-107147.3	1000	-248097.6
1100	38104.7	1100	-44749.6	1000	-157453	1100	-25613.4	1100	-61478.2	1100	-120597.9	1050	-100309.8	1050	-242716.2
1150	41000.7	1150	-42816.6	1039.65	-153318	1150	-21560	1150	-57751.7	1150	-116096.8	1100	-93512.4	1100	-237343.1
1200	43894.5	1200	-40899.3	1039.65	-153318	1200	-17525.1	1200	-54053.7	1200	-111612.9	1150	-86731.7	1150	-231978.8
1233.95	45859.2	1250	-38995.2	1050	-151250	1250	-13508	1250	-50383.5	1250	-107145.6	1200	-79953.2	1181.47	-228606.7
1233.95	45859.2	1300	-37102	1100	-141278	1300	-9507.8	1300	-46740.1	1300	-102694.7	1250	-73167.4	1181.47	-228606.7
1250	47082.4			1150	-131341							1300	-66367.8	1200	-224817
1300	50897.8			1200	-121437									1250	-214610.8
				1250	-111567									1300	-204435.4
				1300	-101729										

Pb + 0.5 O2 = PbO		Hg + 0.5 O2 = HgO		Ni + TiO2 + 0.5 O2 = NiTiO3		2 NbO2 + 0.5 O2 = Nb2O5		Co + 0.5 SiO2 + 0.5 O2 = 0.5 Co2SiO4		2/3 Fe + 1/3 Ca2Fe2O5 + 0.5 O2 = 2/3 CaFe2O4	
300	-189108.1	300	-58306	T	ΔG	T	ΔG	T	ΔG	T	ΔG
350	-184080.3	350	-52901.5	300	-228589.4	300	-287346.2	300	-226853.4	300	-248487.3
400	-179097.3	400	-47523.9	350	-223756.5	350	-283645	350	-222774.5	350	-244196.6
450	-174162.5	450	-42182.3	400	-218954.8	400	-279962.9	400	-218740.4	400	-239952.3
500	-169275.8	500	-36882.4	450	-214178.3	450	-276299.1	450	-214754.2	450	-235740.7
550	-164435.6	550	-31626.8	500	-209419	500	-272651.8	500	-210814.6	500	-231552.2
600	-159639.3	600	-26417	550	-204668.5	550	-269018.3	550	-206918.1	550	-227380.1
600.6	-159582	630.57	-23253.9	600	-199917.1	600	-265394.7	600	-203059.6	600	-223218.7
600.6	-159582	630.57	-23253.9	650	-195154.2	650	-261776.4	650	-199233.9	650	-219063.3
650	-154489.8	650	-19430.7	700	-190392.4	700	-258158.2	694.99	-195814.4	700	-214910
700	-149371.6	700	-9639.1	750	-185641	750	-254534.4	694.99	-195814.4	750	-210755
750	-144288.8	750	85.4	800	-180901.6	800	-250898.8	700	-195431.6	800	-206594.6
771.96	-142067.8	800	9745.5	850	-176174.7	850	-247245.3	750	-191621.8	850	-202425.2
771.96	-142067.8	811.67	11991.9	900	-171460.3	900	-243567.6	800	-187825.6	900	-198242.8
800	-139244	811.67	11991.9	950	-166758.4	950	-239859.6	848.01	-184187.1	950	-194043
850	-134229.6	850	13507.6	1000	-162068.7	1000	-236115.1	848.01	-184187.1	1000	-189820.3
900	-129241.1	900	15487.3	1050	-157391.3	1050	-232328.5	850	-184035.5	1050	-185567.8
950	-124279	950	17469.6	1100	-152725.8	1087.81	-229433.5	900	-180240.5	1100	-181290.3
1000	-119343.9	1000	19454.3	1150	-148072.1	1087.81	-229433.5	950	-176458.5	1150	-176999.9
1050	-114436.1	1050	21441.5	1200	-143430.3	1100	-228418.6	1000	-172685.8	1184.81	-174007.9
1100	-109556.1	1100	23431.2	1250	-138800.1	1150	-224221.7	1050	-168919	1184.81	-174007.9
1150	-104704.1	1150	25423.2	1300	-134181.5	1200	-219966.2	1100	-165154.3	1200	-172693.9
1159	-103833.7	1200	27417.6			1250	-215674.7	1140.09	-162134.7	1250	-168371.2
1159	-103833.7	1250	29414.4			1300	-211373.9	1140.09	-162134.7	1300	-164054.3
1200	-100786.9	1300	31413.4					1150	-161379.2		
1250	-97106.1							1200	-157561.5		
1300	-93462							1250	-153733.4		
								1300	-149890.6		

1/3 MnO + 2/3 Fe + 0.5 O2 = 1/3 MnFe2O4		0.5 Cu + 0.5 MoO2 + 0.5 O2 = 0.5 CuMoO4		CO + 0.5 O2 = CO2		2/3 In + 0.5 O2 = 1/3 In2O3	
T	ΔG	T	ΔG	T	ΔG	T	ΔG
300	-253275.4	300	-138991.4	300	-257114.8	300	-276388.5
350	-248827	350	-135186.9	350	-252775.8	350	-271079.5
400	-244418	400	-131416.1	400	-248402.6	400	-265789.6
450	-240051.7	450	-127680	450	-244009.9	429.76	-262650.1
500	-235729	500	-123978	500	-239607	429.76	-262650.1
550	-231449.2	550	-120309.2	550	-235200.3	450	-260416.1
600	-227213.1	600	-116672.2	600	-230794.2	500	-254911.2
650	-223018.6	650	-113066.1	650	-226391.6	550	-249427
700	-218857.4	700	-109489.6	700	-221994.4	600	-243963.8
750	-214721.6	750	-105942.1	750	-217604	650	-238521.1
800	-210604	800	-102422.7	800	-213221.4	700	-233098.4
850	-206498	850	-98930.9	850	-208847.1	750	-227695
900	-202396.6	900	-95466.3	900	-204481.5	800	-222310
950	-198292.9	950	-92028.7	950	-200124.9	850	-216942.7
1000	-194179.3	1000	-88617.9	1000	-195777.4	900	-211592.5
1050	-190046.9	1050	-85233.9	1050	-191439.1	950	-206258.5
1100	-185898.4	1100	-81876.8	1100	-187110.1	1000	-200940.2
1150	-181744.3	1150	-78546.6	1150	-182790.1	1050	-195636.9
1184.81	-178850.8	1200	-75241.6	1200	-178479.3	1100	-190348.1
1184.81	-178850.8	1250	-71958.7	1250	-174177.4	1150	-185073.4
1200	-177580.5	1300	-68694.8	1300	-169884.4	1200	-179812.2
1250	-173404.3					1250	-174564.2
1300	-169236.9					1300	-169329.1

Ti2O3 + 0.5 O2 = 2 TiO2		WO2 + 0.5 O2 = WO3		Pr2O3 + 0.5 O2 = 2 PrO2		BeO + WO2 + 0.5 O2 = BeWO4		0.5 Ni + 0.5 WO2 + 0.5 O2 = 0.5 NiWO4		0.5 Fe + 0.5 WO2 + 0.5 O2 = 0.5 FeWO4	
T	ΔG	T	ΔG	T	ΔG	T	ΔG	T	ΔG	T	ΔG
300	-344960.5	300	-230075.6	300	-59535.3	300	-291770.8	300	-244762.4	300	-274741.1
350	-341024.3	350	-226230.3	350	-54681.8	350	-287853.2	350	-240785.9	350	-270974.4
400	-337094.3	400	-222406.2	400	-49954.6	400	-283942	400	-236832.7	400	-267215.1
450	-333123.2	450	-218605	450	-45358.2	450	-280035.7	450	-232889.1	450	-263453.3
469.98	-331510.7	500	-214828.5	500	-40892	500	-276133.6	500	-228945.7	500	-259683.1
469.98	-331510.7	550	-211077.1	550	-36553.3	550	-272236	550	-224995.2	550	-255900.6
500	-328991.7	600	-207350.5	600	-32338.6	600	-268343.5	600	-221031.2	600	-252103.5
550	-324753.2	650	-203647.7	650	-28244.1	650	-264457.1	650	-217047.8	650	-248290.3
600	-320462.7	700	-199967.6	700	-24266.3	700	-260578.1	700	-213051.1	700	-244459.6
650	-316122.7	750	-196308.6	750	-20401.8	750	-256708.1	750	-209045.9	750	-240610.6
700	-311735.6	800	-192669.3	800	-16647.4	800	-252848.8	800	-205033.4	800	-236742.2
750	-307303.7	850	-189048.4	850	-13000.4	850	-249002	850	-201014.1	850	-232853.3
800	-302829.1	900	-185444.8	900	-9458.2	900	-245169.7	900	-196988.7	900	-228942.5
850	-298313.8	950	-181857.6	950	-6018.4	950	-241353.8	950	-192957.7	950	-225008.1
900	-293759.4	1000	-178286.1	1000	-2678.8	1000	-237556.3	1000	-188921.6	1000	-221047.2
950	-289167.5	1050	-174729.9	1050	562.3	1050	-233779.1	1050	-184881	1050	-217056.2
1000	-284539.4	1050	-174729.9	1100	3706.9	1100	-230024.1	1100	-180836.2	1100	-213039.7
1050	-279876.3	1050	-174729.9	1150	6757.5	1150	-226293	1150	-176787.9	1150	-209008.1
1100	-275179.4	1100	-171254.3	1200	9720.4	1200	-222587.6	1200	-172736.5	1184.81	-206194.9
1150	-270449.7	1150	-167783.5	1250	12602.1	1250	-218909.5	1250	-168682.4	1184.81	-206194.9
1200	-265688.1	1200	-164318	1300	15408.7	1300	-215260.2	1300	-164626.3	1200	-204960.5
1250	-260895.4	1250	-160858.1							1250	-200897
1300	-256072.6	1300	-157404.1							1300	-196835.4

MnO + WO2 + 0.5 O2 = MnWO4		2 CeCrO3 + 0.5 O2 = Cr2O3 + 2 CeO2		2 Cu + Al2O3 + 0.5 O2 = Cu2Al2O4		Ni + Cr2O3 + 0.5 O2 = NiCr2O4		Ni + 0.5 SiO2 + 0.5 O2 = 0.5 Ni2SiO4	
T	ΔG	T	ΔG	T	ΔG	T	ΔG	T	ΔG
300	-308688.3	300	-195793.6	300	-168359.6	300	-220770.7	300	-214916.8
350	-305108.6	350	-190480.2	350	-164012.8	350	-216375.5	350	-210464.9
400	-301575.3	400	-184909.6	400	-159671.4	400	-211992.9	400	-206016.8
450	-298069.3	450	-179176	450	-155342.1	450	-207634.9	450	-201577.5
500	-294578.8	500	-173340.4	500	-151028.1	500	-203299.2	500	-197146.6
550	-291097	550	-167435.8	550	-146731.2	550	-198979.2	550	-192719.9
600	-287619.9	600	-161482.2	600	-142452.5	600	-194665.9	600	-188289.9
650	-284146	650	-155493.4	650	-138192.3	650	-190348.8	650	-183846.4
700	-280675.2	700	-149479.1	700	-133950.9	700	-186039.9	700	-179400.9
750	-277207.8	750	-143446.4	750	-129728.1	750	-181748.2	750	-174961
800	-273744	800	-137400.6	800	-125523.9	800	-177474.4	800	-170525.5
850	-270284.6	850	-131344.8	850	-121337.8	850	-173218.3	848.01	-166268.2
900	-266830.7	900	-125280.9	900	-117169.5	900	-168979.3	848.01	-166268.2
950	-263383.6	950	-119210	950	-113018.4	950	-164756.6	850	-166090.8
1000	-259944.6	1000	-113133.2	1000	-108883.8	1000	-160549.2	900	-161649.5
1050	-256515.1	1050	-107051.2	1050	-104765.2	1050	-156356.5	950	-157222.1
1100	-253096.5	1100	-100964.5	1100	-100662.3	1100	-152177.5	1000	-152807.7
1150	-249690.1	1150	-94873.6	1150	-96574.9	1150	-148011.6	1050	-148405.5
1200	-246297.3	1200	-88778.9	1200	-92503.4	1200	-143858	1100	-144014.4
1250	-242919.4	1250	-82681.4	1250	-88446.9	1250	-139716	1140.09	-140500.7
1300	-239557.7	1300	-76585	1300	-84404.7	1300	-135585.1	1140.09	-140500.7
								1150	-139624.4
								1200	-135206.3
								1250	-130795.6
								1300	-126391.4

Co + Cr2O3 + 0.5 O2 = CoCr2O4		MnSiO3 + 0.5 O2 = MnO2 + SiO2		MnAl2O4 + 0.5 O2 = MnO2 + Al2O3		Cd + H2O + 0.5 O2 = Cd(OH)2	
T	ΔG	T	ΔG	T	ΔG	T	ΔG
300	-283085.1	300	-74384.7	300	-76141.5	300	-236414.8
350	-278542.9	350	-68870.6	350	-70543.9	350	-229879.8
400	-274063	400	-63343.6	400	-64929.2	373.5	-226727.3
450	-269645.1	450	-57814.9	450	-59315.1	373.5	-226727.3
500	-265281.3	500	-52295.5	500	-53713.3	400	-220255.5
550	-260963.7	550	-46795.2	550	-48131.2	450	-208081.7
600	-256685.3	600	-41322.2	600	-42573.9	500	-195947.9
650	-252440.3	650	-35883.6	650	-37044.6	550	-183843.2
694.99	-248645.2	700	-30486.1	700	-31545.5	594.22	-173155.1
694.99	-248645.2	750	-25135.9	750	-26077.7	594.22	-173155.1
700	-248220.7	800	-19839.2	800	-20641.9	600	-171698.4
750	-243997.6	848.01	-14810.1	850	-15238.4	650	-159105.3
800	-239794.8	848.01	-14810.1	900	-9867.2	700	-146520.2
850	-235608.8	850	-14603.7	950	-4528.1	750	-133939.5
900	-231436.4	900	-9443.4	1000	779.3	800	-121360.4
950	-227274.6	950	-4315.1	1050	6055.5	850	-108780.1
1000	-223120.7	1000	781.8	1100	11301	900	-96196.4
1050	-218971.6	1050	5848.1	1150	16516.6	950	-83607.4
1100	-214824.7	1100	10884.7	1200	21702.8	1000	-71011.2
1150	-210676.8	1140.09	14902.5	1250	26860.3	1035.22	-62133.3
1200	-206524.8	1140.09	14902.5	1300	31989.9	1035.22	-62133.3
1250	-202365.2	1150	15874.4			1039.65	-61788.7
1300	-198194.2	1200	20762			1039.65	-61788.7
		1250	25621.2			1050	-59993.3
		1300	30453			1100	-51348.8
						1150	-42750.9
						1200	-34198
						1250	-25688.8
						1300	-17221.8